FINAL REPORT

Influence of Fuel Heterogeneity and a Novel Fuel Rendering Technique on Fire Spread Predictions

SERDP Project RC19-1329

OCTOBER 2020

Eric Rowell
Kevin Hiers
Louise Loudermilk
Scott Goodrick
Tall Timbers Research Station

SERDP
DOD ▪ EPA ▪ DOE

REPORT DOCUMENTATION PAGE

Form Approved
OMB No. 0704-0188

1. REPORT DATE *(DD-MM-YYYY)*	**2. REPORT TYPE**	**3. DATES COVERED** *(From - To)*
15-April-2020	SERDP Final Report	24April2019 – 24April2020

4. TITLE AND SUBTITLE

Influence of fuel heterogeneity on fire spread models

5a. CONTRACT NUMBER
W912HQ19P0031

5b. GRANT NUMBER

5c. PROGRAM ELEMENT NUMBER

6. AUTHOR(S)

Eric Rowell, Kevin Hiers, Louis Loudermilk, and Scott Goodrick

5d. PROJECT NUMBER
RC19-1329

5e. TASK NUMBER

5f. WORK UNIT NUMBER

7. PERFORMING ORGANIZATION NAME(S) AND ADDRESS(ES)

Tall Timbers Research Station
13093 Henry Beadel RD
Tallahassee, FL 32312

USFS Southern Research Station
320 E. Green St
Athens, GA 30602

8. PERFORMING ORGANIZATION REPORT NUMBER

RC19-1329

9. SPONSORING / MONITORING AGENCY NAME(S) AND ADDRESS(ES)
Strategic Environmental Research and Development Program

10. SPONSOR/MONITOR'S ACRONYM(S)
SERDP

11. SPONSOR/MONITOR'S REPORT NUMBER(S)
RC19-1329

12. DISTRIBUTION / AVAILABILITY STATEMENT

UU(Unclassified Unlimited)

13. SUPPLEMENTARY NOTES

14. ABSTRACT

The overarching objective of this limited scope proposal is to quantify the sensitivity of fire spread predictions to the level of spatial detail found in novel 3D fine-scale surface fuels measurements. This is important because numerical-based coupled fire-atmosphere models produce highly resolved predictions of fire behavior, but have been limited by oversimplified fuels data and fuel models. Testing the efficacy of terrestrial and airborne laser scanning fuel metrics, we us Shannon's Diversity Index to assess the effect on scale as a function of information loss. We develop an automated 3D fuels litter simulation to evaluate fine-scale variability of

15. SUBJECT TERMS
Fuel heterogeneity, fire spread models, Airborne Laser Scanning, Frequently burned systems, Fuels, HIGRAD\FIRETEC QUIC-fire, Simulated 3D fuels, Shannon's diversity index, Terrestrial Laser Scanning

16. SECURITY CLASSIFICATION OF:			**17. LIMITATION OF ABSTRACT**	**18. NUMBER OF PAGES**	**19a. NAME OF RESPONSIBLE PERSON**
a. REPORT	**b. ABSTRACT**	**c. THIS PAGE**			Eric Rowell
Non-Classified	Non-Classified	Non-Classified	UU	61	**19b. TELEPHONE NUMBER** *(include area code)* 406-396-6736

Standard Form 298 (Rev. 8-98)
Prescribed by ANSI Std. Z39.18

Table of Contents

Keywords

Airborne Laser Scanning

Frequently burned systems

Fuels

HIGRAD\FIRETEC

QUIC-fire

Simulated 3D fuels

Shannon’s diversity index

Terrestrial Laser Scanning

List of Tables

List of Figures

from increased needle count may just be a statistical effect. In other words, higher needle counts increase the chance of a falling needle filling an opening in the litter stack but does not mean a change in litter structure after a certain point.

Figure 19: Ensemble run results for classic fire behavior metrics. Ensemble run results for a) burned area (m2) at simulation end time (t=400 s), b) max rate of growth (m2/s) and c) max rate of spread (m/s). Error bars are calculated by using the 90th percentile.

Figure 20: Fuel consumption variety at simulation end time. Fuel density at simulation end time for the a) min, b) median, and c) max of burned case scenario for a low resolution, high wind, low moisture run.

Figure 21: Fire behavior at different levels of fuel resolution. Fuel density at the surface level for a low wind / low moisture condition for a) 2m, b) 4m, c) 8m, d) 16m, e) 32m, and f) single characteristic.

Figure 22: Ensemble run results for the reduced area. Error bars are calculated by using the 90th percentile from the ensemble runs. X-axis represents the scale at which the fuels were aggregated prior to the run starting.

Figure 23: Ensemble run results for the max RoS/BRoS for all conditions. Error bars are calculated by using the 90th percentile from the ensemble runs. X-axis represents the scale at which the fuels were aggregated prior to the run starting.

Figure 24: Ensemble run results for the normalized canopy consumption. Error bars are calculated by using the 90th percentile from the ensemble runs. X-axis represents the scale at which the fuels were aggregated prior to the run starting.

Figure 25: Results for surface fuel aggregation as opposed to aggregation of all vertical layers. Ensemble run results for a) burned area (m2) at simulation end time (t=400 s), b) max rate of growth (m2/s) and c) normalized canopy consumption () for all runs. Error bars are calculated by using the 90th percentile from the ensemble runs. In pink, cyan and lime green are shown the single run results for runs averaging only the surface fuels.

Figure 26. Surface and canopy consumption for a surface fuel aggregation. Surface fuel density at simulation end time for a) a 2m resolution run, c) a single characteristic run, and fraction canopy fuel remaining for b) 2m resolution run, d) single characteristic run.

Figure 27. Shannon diversity index for different categorization schemes

Figure 28. Results of diversity index as output variable. Shannon diversity index for fuel density at simulation end time as a function of the detailed fuel moisture diversity index.

Figure 29. Ensemble run results for maximal downwind spread (m). Error bars are calculated by using the 90th percentile from the ensemble runs. X-axis represents the scale at which the fuels were aggregated prior to the run starting.

Figure 30. Percent change in Shannon diversity index as a function of the scale of resolution of the fuel information for the 4 highest intensity fires from Table 4.

Figure 31. Percent change in Shannon diversity index as a function of the scale of resolution of the fuel information for the 4 lowest intensity fires from Table 4.

List of Acronyms

3D - three-dimensional

AGB –Aboveground biomass

AFB- Air Force Base

ALS – Airborne Laser Scanning

CFD - Computational Fluid Dynamics

DoD - Department of Defense

EAFB - Eglin Air Force Base

HIGRAD/FIRETEC- A coupled atmosphere and physics- and fluid dynamics-based fire behavior model.

LOOCV- Leave-One-Out-Cross-validation

RxCADRE - Prescribed Fire Combustion and Atmospheric Dynamics Research Experiment

SE – Southeastern

SAV- Surface area to volume ratio.

TLS - Terrestrial Laser Scanning

QUIC-FIRE- A hybrid cellular automated and physics-based fire behavior model.

Acknowledgements

Thanks to Daniel Rosales-Giron who performed analyses for the QUIC-fire simulation and David Robinson who performed the fuel simulation development. Christie Hawley who developed the 3D fuels clip plot protocols.

Abstract

Objective: The objectives of this limited scope were to evaluate the effects of spatial scaling in computational fluid dynamics (CFD) based fire behavior models as relevant to changes in coarsening fuels inputs coupled with changes in wind speed and fuel moisture. Decision making for prescribed fire planning is a challenge with the current portfolio of fire behavior modeling as characterization of fire behavior is generalized, coarse in scale, and has high uncertainty in estimates of smoke production that is critical to burn planning on DoD lands. The approach described in this limited scope project leverages a new quick solving\cellular automata model, QUIC-FIRE, to begin testing assumptions of scale that could have impacts on how DoD managers utilize this emerging tool. This was a "high-risk" project because there has been limited development of quantifiable high resolution fuels data until recently, the model at time of the proposal was still in the development stage, and the inclusion of highly realistic fuelbed simulations could improve characterization of intrinsic fuel properties (e.g. surface area to volume ratio and bulk density) that play critical roles in how CFD models propagate fire across landscapes.

Technical approach: Improvements in the characterization of surface fuelbeds through the development of new methods of analyzing terrestrial and airborne laser scanning systems have advanced the discipline of fuels science. We employ two modes of data from these systems, describing a new novel approach of fuels characterization using terrestrial laser scanning (TLS) estimates of porosity and surface area. We also employ methods to use TLS–based fuels estimates to predict landscape scale fuels from airborne lidar scanning (ALS). These data were used to test scaling effects of fuels, wind, and fuel moisture within the QUIC-FIRE model at two test sites, Pebble Hill Plantation in south Georgia and Eglin Air Force Base in Florida, USA. Multiple and ensemble simulations were compared between scales and environmental factors to evaluate optimal scales of fuels inputs. Using diversity indices from information theory, this study sought to identify thresholds where no additional information is lost as scale coarsens. Information loss is evaluated as a function of both inputs and fire behavior outputs.

Results: Generation of fuels inputs from TLS and ALS data sources demonstrate that robust characterization of fine-scale fuel variables as bulk density can be integrated as inputs to CFD models. The aggregation of these fuels input and subsequent modeling simulations describe information loss that indicates specific ranges of fuel scale that may be determined as the maximum threshold of scale for fuel characteristics. Scales that exceeded 20m voxel scale indicated that most or all of the information had been lost as compared to finer scales suggesting that there is limited advantage to using coarse scale data if understanding the impact of higher resolution fire model outputs as rate and shape of spread, energy release, and consumption are important metrics. We also investigated the ability to improve and automate the characterization of three-dimensional fuelbeds using high fidelity plant and fuel particle models with an improved method to distribute pine litter across landscape that also includes model estimates of critical intrinsic fuel properties.

This limited scope project identifies several technical considerations and improvements for deriving, scaling, and assessing CFD modeled fire dynamics and effects. The short duration of the project necessitated using existing "realistic" fuelbeds from TLS and ALS data, however there was uncertainty regarding fire spread as function of the model or fuels characterization. We also identify that more work needs to be conducted in characterizing the fire energy outputs using spatial entropy as opposed to only a diversity index to better understand the links between input scale and expected outputs. The ability to describe fuels through the simulated fuelbeds method unveiled multiple limitations for implementation based on complexity and resolution of the models. Future research in this domain should focus on the trade-offs between resolution and efficiency of distribution and characterization of these fuel elements across large spatial domains.

Benefits: Improvements of CFD-based fire behavior models requires robust and scalable fuels inputs across DoD lands for better planning and monitoring of prescribed fire. Remotely sensed data is the critical link characterizing fuels across DoD landscapes and the scales described in this project are useful to determining levels of data scale that will meet the needs of managers as they start employing CFD models in their strategic portfolio. The results of this project also have impact in regards to sources of data that need to be available to manages and researchers alike. Generalized fuels representation from national repositories are two-dimensional and treat the surface fuels in homogenous categories, thus some level of finer-scale fuels are important to scale to larger landscape scale datasets.

Objective

A seldom tested aspect of computational fluid dynamics (CFD) fire behavior models is the effect of model sensitivity to changes in scale of the fuel representation. This issue of input scale is due in part to the lack of realistic representation of fine detail of heterogeneous fuels from remote sensing, as well as the computational cost of ensemble modeling required to explain the resulting changes in fire behavior. It is expected that as the scale of a three-dimensional voxel increases, the amount of information carried from one scale to the next reduces to the point of an information threshold (Altieri et al. 2017). From this point on, there is no discernable increase in information and we can then assume that there is an optimal maximum scale that exists for large-scale modeling. The primary innovation of Altieri et al (2017) is that entropy can be decomposed into a term accounting for the role of space and a noise term summarizing the residual information (spatial mutual information and spatial residual entropy). The theme of information exchange frames our research, where tactical decisions of input scale from multiple data sources drive assumptions of expected fire behavior model outputs.

Figure 1. The primary themes of the study and the workflow of RC-19-1329

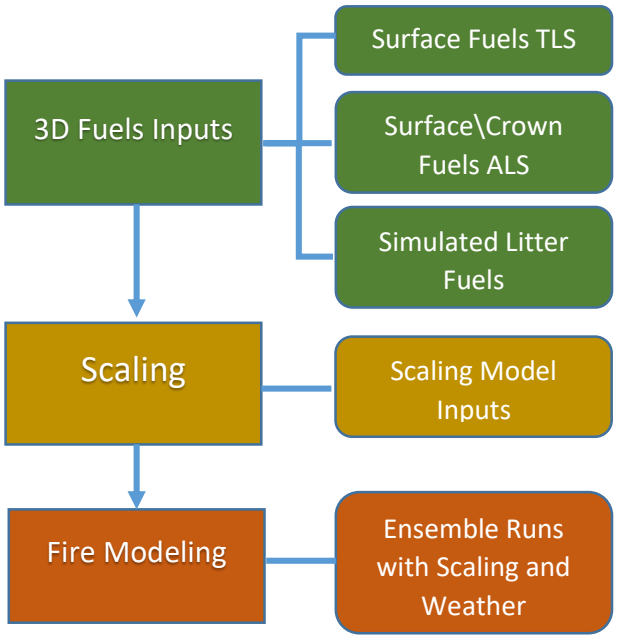

For the purposes of this final report, we divide the themes into three divisions, 3D fuels inputs (**Fig 1**, green box), scaling (**Fig. 1**, yellow box), and fire behavior modeling. To begin automating simulated fuelbeds across landscapes, we first improved the methods to describe bulk density of TLS characterization of fuelbeds by developing an expandable method. We then tested the capabilities of the QUIC-fire model that may influence scale-fire behavior interactions, including: 1) scaling lanes of fuel, moisture, and wind and 2) opportunities to optimize workflow and simulation time that has direct benefit to managers whom will eventually have access to quick-solving fire behavior models. While this report represented the findings of our limited scope efforts, we view this first step of sensitivity analyses to scales of fuels and weather inputs as a benchmark that will drive avenues of future research in the optimization and applicability of next generation fire behavior models. We were also cognizant of this research being applicable to distill relevant conclusions that benefit DoD managers resulting in crosswalks from research to application that are based on sound data and methods (**Table 1**). A major focus of our research project was to determine the optimal 3D resolutions at which surface fuels characteristics effect fire behavior within a quick solving fire behavior model. Our initial assumptions were that derivative outputs (e.g., fire intensity) from the model would provide a diversity of information to explore the effects of changing resolutions. Ultimately, we found that the diversity index we used provided more information when used with the scales of the individual inputs as opposed to the outputs.

The demonstration of proof-of-concept regarding our proposed objectives were to identify the representation of inputs for optimal performance of QUIC-fire fire behavior modeling, quantification of fuel characteristics, differences in methods of 3D fuels characterization, and the use of information theory to determine scale optimization. Meeting these objectives would reduce risk in developing a standard proposal by identifying limitations and opportunities between novel approaches to characterizing three-dimensional fuels and quick solving CFD fire behavior models.

Table 1. Examples of project outcomes and the applicability of these themes for both science and management uses.

Project Activity	Knowledge Acquired	Applicability	Future Uses
TLS	Generate unit\plot based highly resolved heterogeneous fuels	Robust bulk density information for sampling fuels	Sampling framework to improve fuels estimates for managers
ALS	Generates landscape fuel inputs for surface and crown (previously detailed in RC-2243)	Landscape domains that provide structure metrics relevant to managers and affect fluid flow for models	Baseline data used to produce inputs for modeling framework across DoD landscapes
Simulated Fuels	Supplemental fuels input when other 3D data are unavailable	Development of a mechanistic\stochastic model to distribute fuels based on physical models of fuel particles	Alternative baseline data used to produce inputs for modeling framework across DoD landscapes
Scaling	Identification of optimal scale of fuels inputs.	Create optimized 3D fuels inputs for managers to efficiently model prescribed fire	Testing of these scales in other forested ecosystems
QUIC-Fire Ensemble Runs	Rapid solving runs for a variety of environmental conditions and scales.	Allows managers to test a range of conditions to assess optimal outcomes from prescribed fire application	Testing of these ensembles across a wider array of forested ecosystems and integrate terrain effects

Background

Fire is a pervasive mechanism used to manage and maintain fire dependent ecosystems found on DoD installations and nationwide in both public and private lands. Research from large-scale multi-discipline campaigns (e.g., RxCADRE) have produced inputs and potential validation data for CFD models (Ottmar et al. 2016). Inputs, specifically fuels, have generally involved linking 2D traditional fuels inventories with either remotely sensed data or as a representative fuel model that reports fuel properties as a range of expected fire behavior based on intrinsic fuel properties and bulk density. These fuels outputs are typically reported at coarse grainsize due to either the resolution of the remotely sensed data used as an aggregation framework or based on the capacity of the fire behavior model ingesting these data.

The advent of next generation fire behavior modeling has provided a significant opportunity to assess the fire effects that are driven by heterogeneous fuel matrices coupled with dynamic-atmospheric feedbacks (Hilton et al. 2015; Linn et al. 2013). The framework of these

computational fluid dynamics-based (CFD) models have typically been clustered in the domain of Navier-Stokes based solutions to fluid flow coupled to a combustion model that requires large computational resources unavailable to a large user base. As a result, these CFD models have erred towards physical accuracy and depiction of detail at the cost of speed or optimization. The introduction of fast-solving 3D potential flow model with a cellular automata combustion code has created a paradigm of speed with marginal reductions in accuracy associated with full-physics-based CFD models (Linn et al. 2020). The advancement of the fast-solving model QUIC-fire model (Linn et al. 2020) provides a potential avenue for prescribed fire managers to test the effects of complex ignition patterns, a wide variety of dynamic ambient conditions (e.g., wind and moisture), and heterogeneous three dimensional fuel lattices.

Three-dimensional fuels are the unifying element for CFD models. These fuels inputs can be used to test the integration of heterogeneity to simulate fire behavior that then informs future fire effects. Recent advances in fuels science have improved estimation of bulk density by comparing *in situ* measured three-dimensional fuels (Hawley et al. 2019) with voxel based fuel metrics from TLS data demonstrating promising results for unit-wide fuels characterization (Rowell et al. 2020). This advancement in fuels science allows for the direct testing of heterogeneous fuels that are distinguished by fuel type. As fire is a dynamic process driven by incongruities and variability in the fuelbed that are not typically captured in traditional fuels inventories, these new TLS-derived fuel metrics offer an opportunity compare spatial heterogeneity in innovative ways. The separation of litter and grass from shrub dominated fuels allows for fine-grain assessments of fire spread and behavior that are tied directly between bulk density, fuel particle metrics, and fuel moisture. These fuel advancements coupled with findings from information theory evaluations are expected to provide improvements to these emerging fire management tools that will benefit fire managers.

Within the realm of prescribed fire planning, the dominant paradigm has been the use of western-type wildfire inspired models that were designed to meet worst-case scenarios (Hiers et al. 2020). The focus on science investment for western wildfire has not benefited prescribed fire managers whom are tasked with increasingly complex regulatory constraints coupled with altered land use, novel fuels, and climate considerations that come with significant risk (McCullers 2013). Prescribed fire practitioners often rely on personal experience to safely meet resource objectives, yet the before-mentioned advances are key to providing a planning framework that demonstrates direct improvement for operational prediction that support decision-making, achieving objectives, and managing for smoke production (Waldrop and Goodrick 2012; Linn et al. 2020). Thus, evaluating multiscale characterization of vegetation structure is a fundamental inquiry into the resulting effects of prescribed fire (Hiers et al 2009; O'Brien et al. 2018), and requires 3D inputs and new modeling tools for evaluating mechanistic fire effects.

The question of scale is paramount to successfully assessing the efficacy of prescribed fire, specifically in fire effects that are the result of manipulation of conditions (Myanishi and Johnson 2001). Prescribed fires are ignited in conditions that optimize fire behavior to maximize fire effects for specific management objectives and are constantly modified to not exceed desired outcomes (Hiers et al. 2020). For example, frequent intervals of prescribed fire are important for the management of threatened and endangered species as the Red-cockaded woodpecker (Walters et al. 2002). Yet, minimization of high intensity burns that limit cavity tree mortality are also critical to the management of this species. In other prescribed fire systems there may be a different focus that potentially include the consumption of fuel, stand replacement, or modification of forest structure (Mitchell et al. 2009; Gallagher et al. 2017). The underlying principle of integrating the

proper scale of inputs with an ignition pattern and coupled atmospheric fire behavior models is to meet the objectives of a prescribed fire (Hiers et al. 2020).

In a wildfire context, scale of fuel inputs is further challenged by the large scales of the wildfire incident, which now frequently exceed 10000-ha. The scale of fuel inputs that are required to resolve headfire that covers km/day are vastly different than that governing backing fire where most suppression crews work. Thus, understanding information optimization for emerging tools and 3D forest inputs is relevant to all aspect of fire behavior. This report seeks to answer these questions of scale of inputs.

Methods and Materials

3D Fuels Inputs

A. Surface fuels from Terrestrial Laser Scanning

For the laser scanning derived fuels portion of the study, the key objectives were to derive critical bulk density estimates from TLS data for surface fuels, generate a landscape estimate of fuel mass by increasing sample size of fuel observations to improve large domain fuels inputs for scale comparison, and produce a rational canopy fuels layer that affects fluid flow of air parcels that affect fire behavior in the model. We used a dataset collected as part of the Prescribed Fire Consortium experiments conducted at the Pebble Hill Plantation. Terrestrial laser scanning was conducted using a RIEGL VZ2000 to collect three-dimensional point clouds at ~5mm point spacing at 15m range. The VZ2000 is a near infrared eye safe laser that is capable of scanning objects at up to 1000m. Laser scanner collection points were established on the four corners of the rectangular burn units, set back a minimum 2.5m from the unit edge. A single 360° scan was collected in the center of the burn unit. Scan parameters were set to sample points at 0.023° frequency at a scan rate 550 kHz per scan. Individual scans were geospatially located using the onboard GNSS L1 GPS receiver that automatically places all points into the desired spatial reference (UTM 16N, NAD83). From these models to predict fuel mass were developed through comparison with *in situ* 3D clip plots (after Hawley et al 2019) that were collected coincidentally to the TLS data. We initially used the methods described in Rowell (2017) to calculate fuel mass from the TLS data, a voxel occupancy approach that worked well at frequently burned longleaf pine sites at Eglin Air Force Base, Florida. This method tallies occupied 10cm^3 voxels from the TLS data by taking a selected 0.25m^3 column and subdividing the volume into 250000 10 cm^3 cells. Voxel cells that break a threshold of 10 laser points are considered occupied.

Fuel porosity derived from TLS data is a metric similar in practice to packing ratio or as porosity as defined by Anderson (1969). Packing ratio is defined as the fuel load of similar density divided by the fuelbed depth. This metric serves as an estimate of compactness that is critical to explaining how fire propagates through a porous medium. This compactness represents the expected movement of air that affects residence time and combustion intensity (Anderson 1969). The concept of porosity (Anderson 1969) or packing ratio (Rothermel 1972) are terms to describe fuelbed compactness. To replicate this concept, we evaluate the potential of a porosity metric using TLS, we use the definition of porosity as described in Anderson (1969):

$$\lambda \ = 1 - \frac{V_1 - V_2}{\sigma_a V_2} \qquad [1]$$

Where, porosity (λ, ft^3/ft^2) is expressed as a function of fuel be volume (V_1), fuel particle volume (V_2), and fuel particle surface to area volume ratio (σ). For our purposes, we distill the TLS model for porosity as a simple ratio of total available space in a $10cm^3$ voxel ($1000cm^3$) with the occupied volume derived from the TLS data at $1cm^3$ voxel cells for the same voxel domain. We do not include a surface area to volume value for this study, as we are looking to identify metrics that can be directly obtained from the TLS. We expect that calculation of TLS-derived porosity would be well correlated with measured fuel mass.

To test this hypothesis, we calculate TLS-based porosity using equation 1:

$$\lambda = 1 - \frac{\sum OV_{1cm}}{Volume\ 10cm^3} \quad [2]$$

Where, porosity (λ) is the relative proportion of open space resulting from the occupied volume (OV) divided by the total volume of the $10cm^3$ voxel. This assumes that omission and commission errors are the same across voxels. We calculated this definition of fuelbed porosity for the 0-10 cm and 10-20 cm stratum only, as these strata represent where the highest proportion of compact fuels and fuel mass that typically occur in a frequently burned fuelbed (Rowell et al. 2016).

For fuels sampled above 10 cm, we calculated surface area within each occupied voxel. To estimate surface area of fuel elements at the 10 cm3 voxel domain, the points within each voxel were subset and recalculated using a 3D kernel density estimate via the kde3d function included in the misc3d package in R (Tierney 2015). The kernel density function weights distributions of points to subsequently estimate better isosurfaces that can be used to predict surface area (Feng and Tierney 2008). We used the vcgIsosurface function as part of the Rvcg package in R (Schlager 2017) that represents constant densities of the kernel density function over the limits of the voxel domain. This method used the marching cubes algorithm (Lorensen and Cline 1987), that created a surface through intersecting edges of a volume grid with a volume contour. Where edge intersections occur, a vertex was created. The surface area of the fuel element for the voxel domain was calculated using the vcgArea function within Rvcg, which calculates the surface of the triangular mesh from the isosurface. Methods to estimate fuel mass from TLS data have been presented in Rowell et al. (2016) and Rowell (2017,2020). TLS point clouds are integrated into a cohesive data set, normalized to height above ground by subtracting the minimum height, and are then imported into R where the are voxelized at a 10 cm^3 voxel domain across the unit. Above-ground biomass is estimated by using a Leave-One-Out-Cross-Validation linear models for the train function in the caret package (Kuhn 2017) and made a function of the occupied volume of both pre and post fire point clouds.

B. Surface and Crown Fuels from Airborne Laser Scanning

To aggregate fuels from the fine-grain TLS estimates of fuels we utilized the TLS data as training data for multiple linear regression after Hudak *et al.* (2016). In the before mentioned study, a model that The goal of this was to test if increasing the sample size of the selected a 3m radius area around each 1m x 1m plot were reduced to a series of statistical metrics to produce an optimized multiple linear regression to predict surface fuel mass. These metrics are described in Hudak *et al.* (2016) and the model using nine metrics explained 44% of the variability of fuel mass. We replicated this approach by comparing occupied volume based models developed by comparing TLS data with the same two dimensional clip plots at Eglin Air Force Base (Rowell

2017). We produced the ALS estimates of fuel mass by using adapted methods described in Hudak et al. 2016. ALS metrics considered in the predictive modeling included mean height, kurtosis, the return proportion from 0.0 to 0.05 m, mode of returns from 0.0 to 0.5 m, the return proportion from 0.0 to 0.05 m, standard deviation of height for elevations between 0.05 to 0.15 m, standard deviation of height for elevations between 0.15 to 0.50 m, the coefficient of variation for heights between 0.15 to 0.50 m, standard deviation of height for elevations between 0.50 to 1 m, and standard deviation of height for elevations between 1 to 2 m. These ALS metrics were calculated using the CloudMetrics function of FUSION software (McGaughey 2014). TLS derived AGB were binned into training data at a $25m^2$ resolution to facilitate model development using the ALS data. This resolution matches the resolution used by Hudak et al.(2016) with the same ALS dataset. We employed a multiple linear model using the 'lm' function in R. Candidate ALS metrics were thinned to represent "best" regressions using the 'regsubsets' function in the 'leaps' package of R. The Akaike Information Criterion (AIC) statistic was used as the basis for choosing the best subset model. This method was used to generate landscape scale surface fuel mass for the EAFB L2F unit.

Airborne laser scanner data were used alongside software applications described in Silva et al. (2016) to derive individual tree stem locations and attribute necessary parameters such as height and height to live crown (Rowell 2005). ALS returns a height and elevation map, from which tree stem locations can be derived by finding the local maxima of a smoothed height array, and the height assosciated with the local maxima is used as the tree height for that stem. Crown hull, defined as the outer shape of a tree crown when looked from a nadir perspective, is calculated by passing a filter over the gradient of the tree height model. Crown radius is then defined by using the square root of the area of the crown hull. Diameter at base height, which could be parametrized using tree height, has been set as a constant for simplicity since the model is not very sensitive to this variable. Height to live crown is calculated by taking the values for height at the hull of a stem, calculating the mean and standard deviation for these heights, and assigning the height to live crown as the mean minus one standard deviation. These tree inventory variables are all thats needed to populate a canopy and surface fuel domain using the methodology outlined in Linn et al. 2005. The fuel data was then used to run QUIC-Fire, but the surface fuels will be replaced by data measured with Terrestrial Laser Scans (TLS).

Post fire mass estimates are similarly calculated from post fire scans. The output from the algorithm produced summarizations of fuel mass pre-strata allowing estimations of bulk density per strata. These methods were used on the first meter of the fuels and aggregated up to a 0.5 x 0.5 m horizontally and 0.1 m vertically and used as the surface fuels. Data was exported as a list and imported into Python, where the stitching of the surface and canopy fuels occurs.

C. Simulated 3D Fuels

The approach developed by Rowell et al. (2016) used a workflow that generated plant and fuel objects through parametric plant modeling software to a model space where all objects were assembled into a cohesive fuelbed. Disadvantages to this approach were the non-automated process to produce the fuelbeds and the highly resolved and complex geometries of the objects that overloaded computing resources as domain space increased. To address these issues, we integrated an improved workflow to reduce mesh complexity and introduce a method of distributing these fuel objects using combined mechanical and physical processes.

Pine needles were chosen as the first 3D fuel element to explore, as they are the most ubiquitous litter fuel in frequently burned pine ecosystems and have a simple geometry to consider. Once feasibility of the modeling practice was demonstrated, then litter fuels and shrubbery with more complex geometries (pinecones, ferns, etc.) can be modeled and their effects taken into account. Microscopic imagery of pine needle cross-sections from many species show that they have a geometry similar to a triangular prism (**Fig. 2**). Simplifying to a basic geometry adds advantages for the modeling of fuelbeds and subsequent voxelization of the pine needle models. Utilizing a triangular prism for the geometry allows for an analytical expression for the surface area to volume (SAV), that are directly comparable to laboratory measurements of SAV and extract needle dimensions for the 3D models that result in the same individual SAV. Secondly, a triangular prism only has five faces consisting of regular geometry shapes (3 rectangles and 2 equilateral triangles). These five faces provide a water-tight mesh which collision /rigid-body models require to help prevent intersections when objects make contact. More importantly since no further meshing is required we have a computationally efficient shape to model a large number of collisions.

Figure 2. *Pinus strobus* pine-needle cross-section (A) and a triangular prism needle generated in Blender (B).

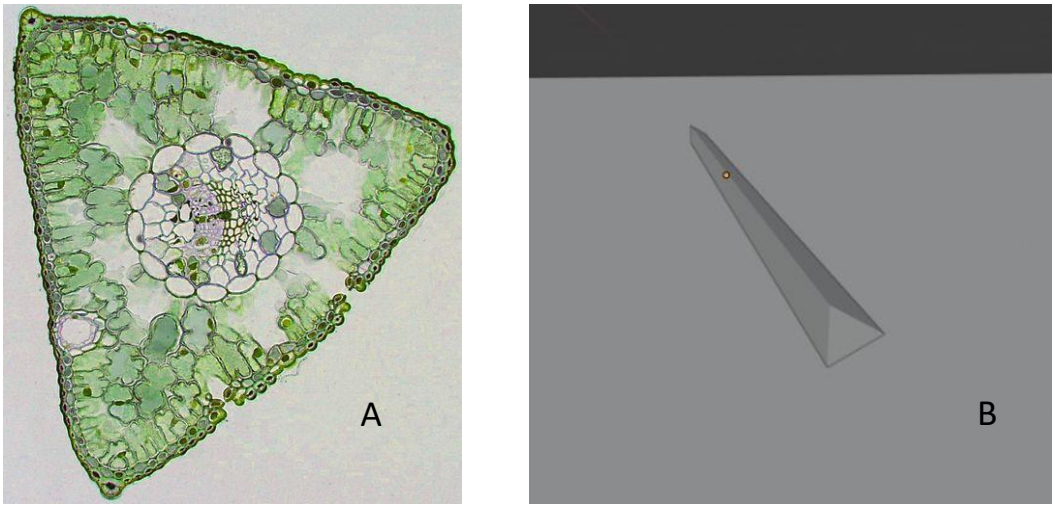

The SAV of a triangular prism can be written as:

$$SAV_{Tri}=2L+43l \quad [3]$$

where L is the long side length of the prism and l is the short side length of the equilateral triangles at each end. Defining the length-to-width ratio LW=Ll we can get the expression:

$$l=2+43LWSAV*LW \quad [4]$$

which gives the short length of the prism as a function of SAV and LW. Longleaf pine needle parameters from Nelson & Hiers (2008) were used with this expression to define the dimensions of the 3D needle models. An SAV of 6071 m^{-1} and LW of 100 results in l=1.1445mm and L=11.4cm (**Fig. 3**).

Figure 3. Curve showing triangular prism dimensions that satisfy an SAV of 6071 m-1.

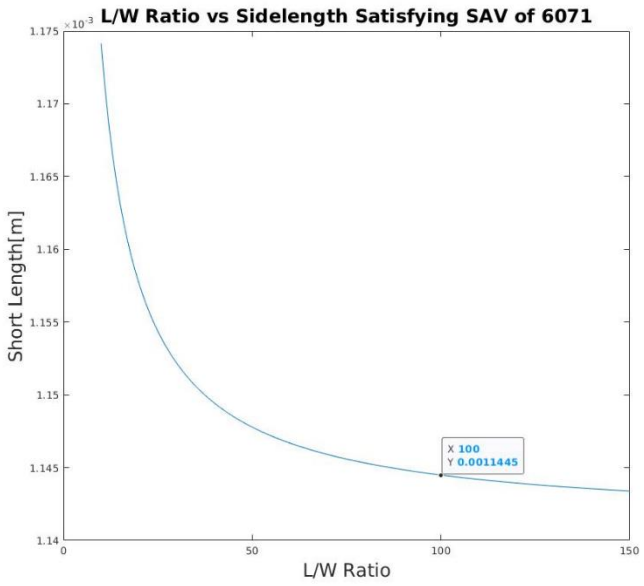

Blender (Blender.org), a free and open-source 3D graphics software, with a rigid body collision algorithm that was used to model the pine needle litter accumulation three-dimensionally. Rigid body collision response is a necessity to simulate interaction among solid objects (Kavan 2003). These algorithms detect collisions and ensure non-penetration of rigid bodies. These algorithms also exploit laws of classical mechanics to optimize speed at the cost of complete physical accuracy (Kavan 2003). To model litter accumulation, we seeded $1m^2$ domains with three increments of needle objects (1000, 5000, 10000, 15000). These objects were randomly distributed above the

Figure 4. Final resting positions of 10,000 needles dropped with random heights and orientations produced by rigid body simulation in Blender.

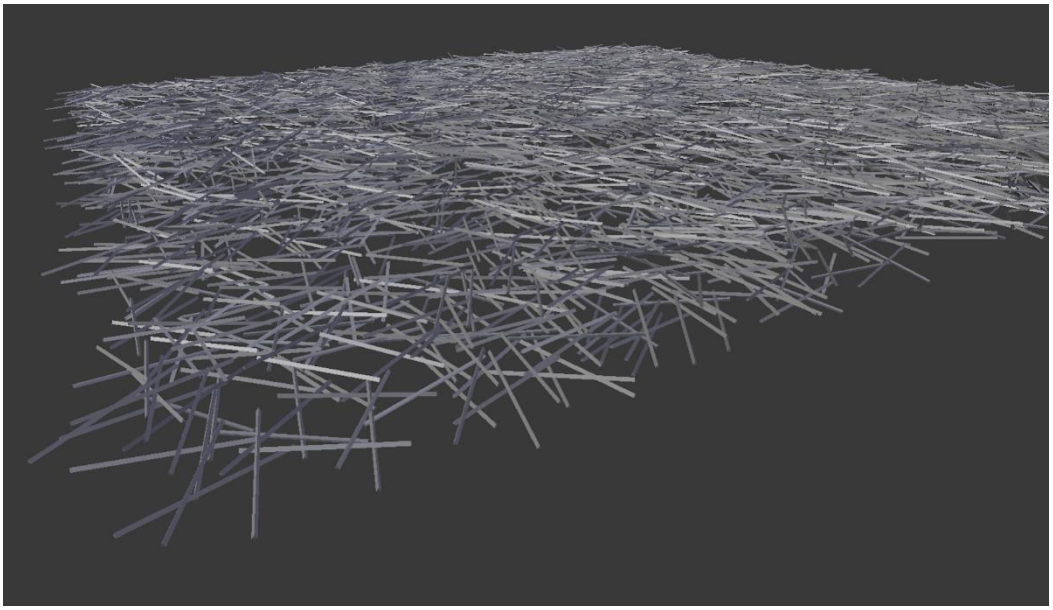

ground plane accounting for position (x,y,z), azimuthal orientation, and elevation angle. The pine needles are dropped from these heights and accelerate at the rate of gravity. Needle objects collide with the ground plane and each other until deaccelerating to a still position. The rigid body response function ensures that objects do not penetrate the surface plane or each other to produce a "realistic" distribution of needle on the ground plane (**Fig. 4**). The model then stores and exports the 3D vertex data of needles.

A scaling factor was introduced due to the small size of the needles. The smallest unit of length that can be handled within Blender is 1.73 *mm,* so all dimensions were scaled by a factor of 10. Not only was this needed so the small side length of 1.15 *mm* could be represented correctly but this also removed an issue of needles intersecting through each other. A uniform distribution was sampled for (*x,y*) position over a 1 *m* x 1 *m* floor in a majority of runs. Results from sampling a one-sided normal distribution are also shown.

Post-Processing

The vertex data from the Blender simulation is voxelized into a uniform 3D cartesian grid. Once a grid is defined, then the vertex data is rescaled back to desired lengths and each individual needle is partitioned into its corresponding voxel volumes. Segmenting needles was done by taking the two center points from the triangular ends and segmenting that line wherever its crossed voxel walls. This allowed for the total needle volume in a voxel to be calculated. The same process was used for each rectangular face on each needle so that surface area from needles could be accurately calculated in each voxel. The voxel location of a triangular face was determined by their center point. Quantities of interest can now be calculated with the accumulated voxel values for surface area and volume. Voxel mass was calculated using a density of 508 kgm^{-3} for the needles (Hough and Albini 1978). Bulk density was calculated by summing all mass in each vertical column then dividing by the max needle height in the column. Porosity was calculated as:

$$\lambda \ = 1 - \frac{\sum NV_{ncm}}{VV\ cm^3} \qquad [5]$$

Where, porosity (λ) is the relative proportion of open space resulting from the occupied needle volume (NV) for n cm within the cubic volume of a voxel. Analysis of fuel heterogeneity within the voxel grid were determined for a range horizontal resolutions (1, 2, 4, 8, and 16 cm*)*. Voxel in the vertical heights were determined as a vertical resolution of two times the shortest length of a pine needle was used (2.289 *mm*).

Scaling for Fire Behavior Modeling

A. Scaling Laser Scanning Inputs

Figure 5: TLS bulk density data as imported into Python. Rotation and cleared out cells are clearly visible

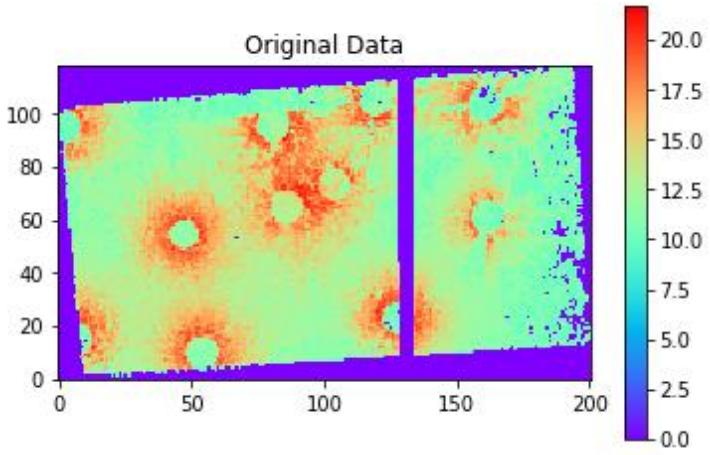

Scaling for both the Pebble Hill and EAFB study site integrated a combination of both TLS and ALS fuel metrics described in preceding sections of the report. For the TLS data collected at the Pebble Hill site, values of bulk density are reported as grams per $0.25m^3$ and are described in three modes of fuel type, litter, grass forb, and shrub dominated. These bulk density values are voxels that can be directly imported into the QUIC-fire environment, though certain considerations need to be addressed before these data were imported into the fire behavior model grid space (**Fig. 5**). Primary issues described are the requirement for the three-dimmensional lattice to be rotated to cardinal directions for the model to produce fire behavior simulations and correcting for any incogruities with the dataset. Data incongruities included missing data that required reconstructung the missing data in a method that did not arbitrarily introduce structures that were inconsistant with populated grid cells.. The original data was also slightly rotated, and the most straightforward fixes such as cropping the entire domain into zones with just data are not applicable. A rotational adjustment was applied to the TLS-based bulk density dataset to integrate these data with a larger model space need to produce "realistic" fluid flow outside of the burn environment. Several interpolation schemes were tested, including spline interpolation schemes of multiple orders. These methods overestimate bulk density in situations of high gradients and would not maintain the representative statistics of the original dataset (**Fig. 6**). The simplest method implemented was a closest neighbor interpolation, which was suitable for both continuous and categorical data, giving reasonably similar results for minimum, maximum, and mean as the original dataset.

Figure 6: Height distributions for surface fuel data. a) Original dataset before rotation, and after implementation of b) low order spline interpolation scheme, and c) closest neighbor *interpolation.*

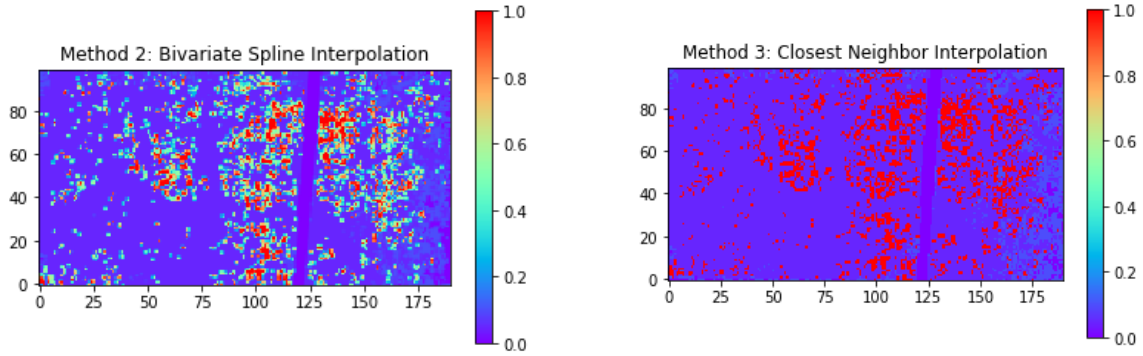

Image reconstruction methods used in remote sensing applications have been built to use neural networks to reproduce data (Zhang et al. 2018), but have not been implemented for this paper. Future work might include such reconstruction efforts. Figure 7, shows the model ready dataset.

The sampling domain for which we have surface fuel data is too small to run QUIC-Fire simulations. With a domain size of 50 x 95 m, and a resolution for QUIC-Fire of 2m, the

Figure 7: Height distributions for surface fuel data. a) Original dataset before rotation, and after implementation of b) low order spline interpolation scheme, and c) closest neighbor *interpolation.*

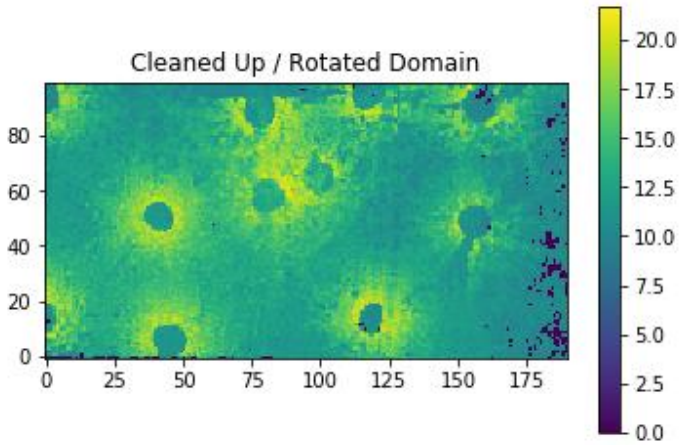

computational domain would be 25 cells long which would lead to edge effects being visible even for a short initial fireline. For these reasons, further methods to extend the domain to a larger area were proposed (**Fig. 8**). The first method attempted was to recursively mirror the original domain into a larger area. This approach ended up introducing large scale structure since the original surface fuel domain had much higher fuel density on the left side of the domain. Mirroring the original domain led to a large area of low fuel density. To avoid large scale structure, the second

Figure 8: Methods used to populate an exterior domain. a) Mirroring original domain, b) using random patches from original domain to populate new domain, and c) using tree inventory data for extended domain.

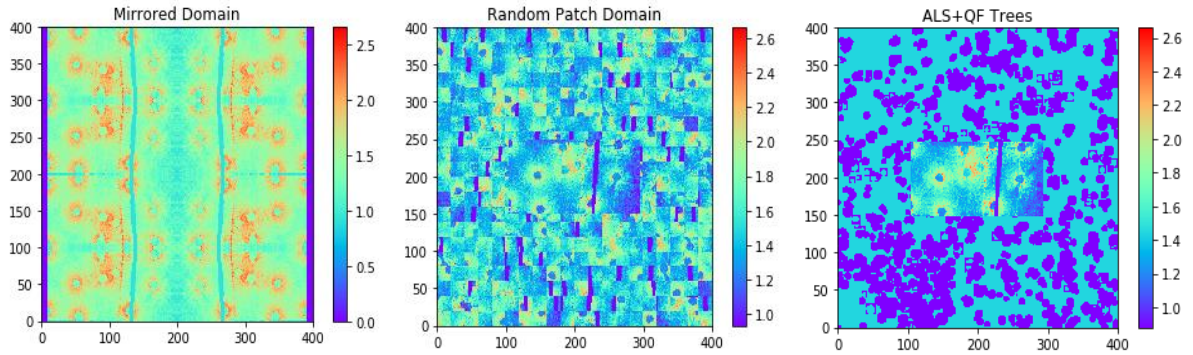

method was to fill the entire domain by randomly selecting 10x10 m patches from the original domain, randomly rotating and placeing patches within the domain. The center of the larger domain is then replaced using the original domain. This was problematic since small scale structure was not maintained. For example if there is a tree on the edge of the selected 10x10 patch, for which some of the trees and biomass were outside of it, this would not be included in the new domain. This resulted in physically impossible situations of floating fuel. The third method to populate the larger domain was to use ALS estimated tree inventory data from the stem detetection algorithm from methods described in (Silva et al 2016) to populate a much larger domain with trees and employ a generalizedgrass and litter model for thesurface fuel data with the voxelized information. This method mantained small and large scale structure and was deemed appropriate since an accurrate tree representation was more valuable for the outside of the TLS domain since canopy cover will influence the effective wind speed on the TLS domain, while surface fuels will not affect it.

Using the TLS data, voxel occupancy is the predictor of the fuel height for each horizontal cell. Categorization of fuel type was estimated using heigh threshholds form the field data, where grass, litter or shrub fuel types represent gradient of heights. Fuels under 10 cm were considered litter, above 10cm but less than 30 cm was considered grass, and anything above 30 cm is categorized as shrubs. This logic was determined based on evaluation of the 3D clip plots collected at the site to parameterize bulk density model. While this does not affect bulk density estimates since those are provided by TLS, it is used to assign fuel moisture content according to environmental conditions. Aggregating to different scales is done by averaging over the appropriate resolution and setting that result to all the cells over which the averaging took place. So, if the resolution that will be used will be 4m, the TLS data is first aggregated up to $2m^3$ cells and then averages are taking on a 2x2 cell basis (4x4 m) and assigned to all the cells that were averaged. If the amount of computational cells does not divide evenly by the averaging length, then the remainder is averaged on a smaller resolution at the edge of the domain. Since the edge of the domain is not expected to burn due to edge effects, this is considered an acceptable practice. Figure 9, shows the results of averaging over different resolutions. It is important to note that averaging occurs at the same scale at every height (z-layer) of the computational domain including the midstory and canopy fuels. Averaging over the canopy fuels means that there will generally be a higher canopy cover, which will reduce the effective wind speed at the surface. Not averaging the canopy fuels

would however not translate to testing out the whole horizontal spatial heterogeneity but just the surface fuel heterogeneity. Future work might address this concerns by looking at results of averaging (or not) layers above the surface fuel. The final step to process fuels is the addition of fuel breaks around the TLS domain. An example of the finalized computational domain at a 2m resolution is shown in figure 10.

Figure 9: Effects of averaging the full domain at different resolutions. a) 1m, b) 4m, c) 16m.

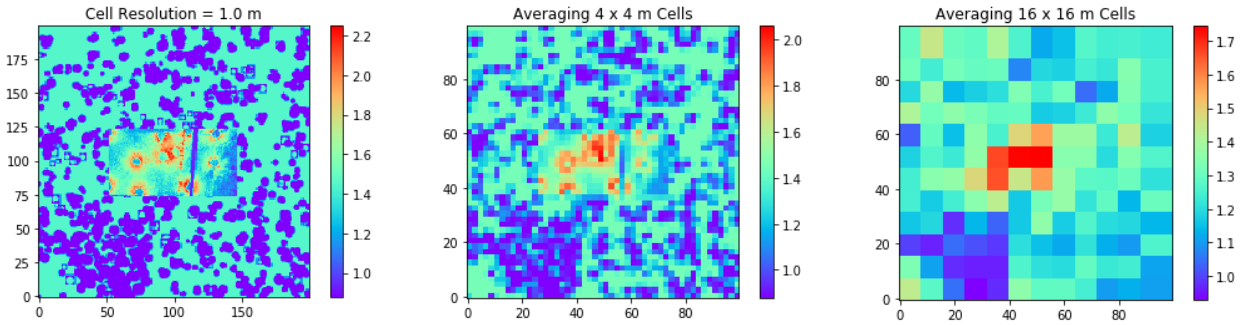

The fire behavior modeling component seeks to evaluate the sensitivity of the model predictions as the level of detail in the fuels data increases under different environmental conditions. The differences in environmental conditions are represented by the fuel moisture content and mean wind speed at 10m and are expected to have large impacts on fire behavior and effects. Fuel moisture scenarios will range from 4%, 8% and 16% for grass fuel moisture conditions for the dry, moderate and moist scenarios, while litter will have a range of 10%, 15%, and 20%, and shrubs will be set permanently at 100%. Wind scenarios will have wind speeds of 3, 6 and 12 miles-per-hour for the low, medium, and high cases, specified at 10m above ground. These scenarios were chosen since the range will be representative of typical conditions for both operational prescribed burns in southeastern pine woodlands. Fuels were aggregated at these scales of resolution: 2m, 4m, 8m, 16m, 32m and a single characteristic plot. Input variables are all stated in Table 2. For the Pebble Hill site, QUIC-Fire was run in an ensemble fashion, with 50 runs for each combination of resolution and environmental condition, in order to leverage the stochastic methods used to calculate fire spread and get a better understanding of the variance on fire behavior effects for each run. Due to the amount of computing time required to run on a larger domain (EAB runs are on a

Figure 10: Finalized computational domain at a 2m resolution.

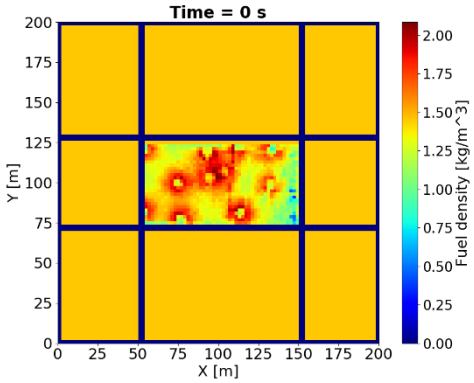

1.5 x 2 km domain, as opposed to 200x200m shown in Figure 10), ensemble runs were limited to a single strip head fire for the EAFB site, where a single seeded run for each environmental condition and resolution level will be used for the analysis section. Ignition is done by lighting two lines 15m downwind from the fuel break going in opposite directions perpendicular to the wind direction, extending down to the end of the TLS domain.

For each run, a suite of fire behavior metrics were calculated to characterize the evolving fire behavior. Maximal downward spread is calculated by measuring the farthest downwind cell where fuel has been consumed. Rate of spread is then calculated by measuring the rate of change of the maximal downward spread. Rate of spread is a valuable metric for fire practitioners and is highly connected to the wind speed felt at the surface, and as such a normalized rate of spread can be calculated by dividing the rate of spread by the wind speed. This will be a way of normalizing runs with different wind conditions. Percent fuel consumption is calculated for the surface and canopy fuels. Surface fuels are defined as being in the first layer of fuel and canopy fuels are defined as everything above that first layer. While further separation and classification of fuels could be done by including midstory fuels, or by analyzing consumption on a per layer basis, since our fuels data has been created by different methods for surface and tree data it seems appropriate to analyze them within those limits too. Canopy consumption is then normalized by the surface fuel consumption. Burned area is calculated as the percentage of cells within the computational domain that have had its fuel partially or fully consumed. Perimeter length is calculated by creating a binary image of the surface fuels in the computational domain depending on if fuel has been consumed there or not, and then counting the amount of cells that are both 'burnt' and have an immediate neighbor that is unburnt. The ratio between these two measures is the reduced area, which measures how close to a circle a shape is. For fire behavior, this metric will measure how evenly outward a fire is spreading. Using the burned area, we can create two more important

Table 2: Input Variable List for QUIC-fire simulations.

Input Variable	Value
Moisture – Grass - Low	4%
Moisture – Grass – Moderate	8%
Moisture – Grass – High	16%
Moisture – Litter - Low	10%
Moisture – Litter – Moderate	15%
Moisture – Litter – High	20%
Moisture – Shrub – All Conditions	100%
Wind Speed – Low	3 mph
Wind Speed – Moderate	6 mph
Wind Speed – High	12 mph
Aggregation Levels	2m – 4m – 8m -16m -32m – Single

metrics: its rate of change over time is the rate of growth, while doing a similar approach at the square root of the burned area gives the bulk rate of spread. The bulk rate of spread is meant to represent the average rate of spread of the fire, and can be expressed as a ratio with the rate of spread to represent how much of the fire is represented by the head fire, as opposed to the backing and flanking sections of the fire. These metrics are important for different reasons and all aim to represent different aspects of fire behavior.

Shannon's diversity index was used to measure the level of homogeneity in both the fuel input data and the fuel consumption data output. Shannon's diversity index is calculated by classifying data into selected categories and calculating the evenness of proportions across those categories and is used in data science as a measure of the information content being placed into the model and the output of the model.

$$H = \frac{nlog(n) - \sum_{i=1}^{k} filog(fi)n}{n} \quad [6]$$

Where *k* and n denote the number of groups and the total count, f_i the vector of frequencies (count) Shannon diversity. If f_i=0, then the f_i log(f_i) term is set to 0. Two different category systems were selected for the fuel input model and one category system for the output. Fuel density was classified by taking the minimum and the maximum at the 2m resolution level and making 20 categories between those two. Fuel moisture was classified by making three categories depending on fuel height, since the fuel height dictated the fuel moisture. It was then a measure of evenness between grass, litter, and shrub moisture contents. Output fuel density was classified with a simple

Figure 11: Fuel density at six different scales of resolution.

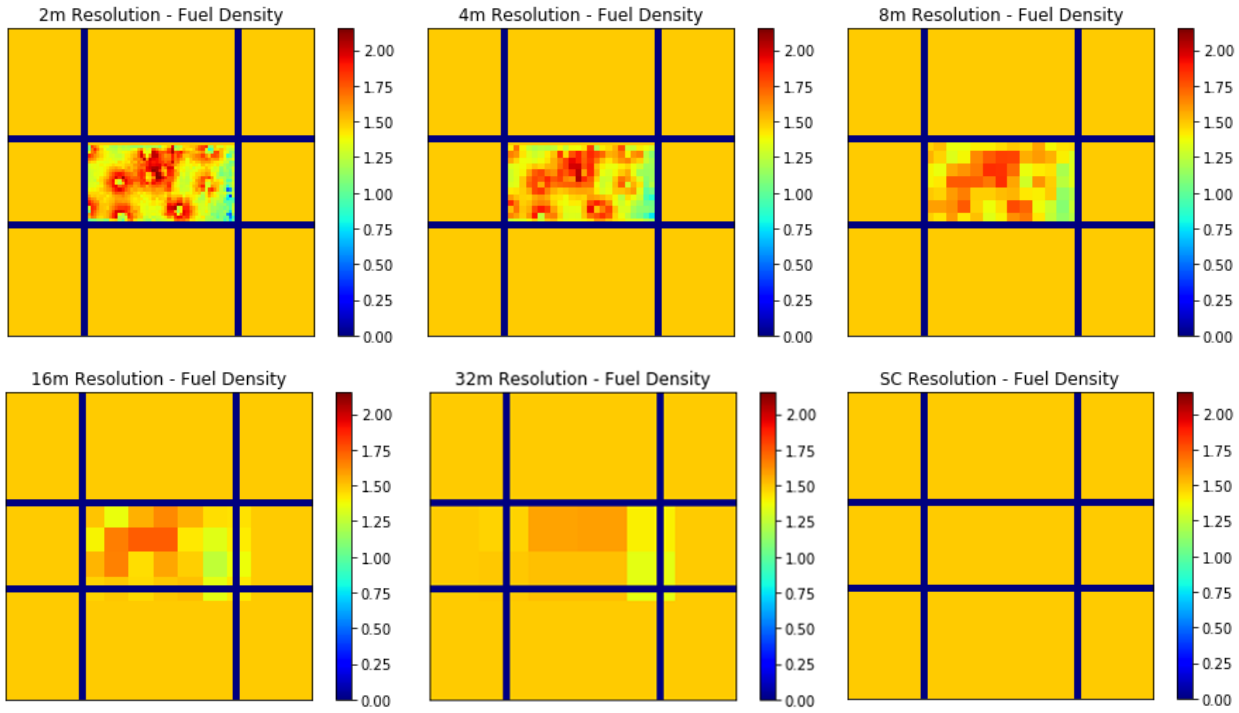

burnt/unburnt dichotomy. The initial fuel density (**Fig. 11**) and fuel moisture (**Fig. 12**) for different levels of resolution were compared using Shannon's diversity index.

Figure 12: Fuel moisture at six different scales of resolution.

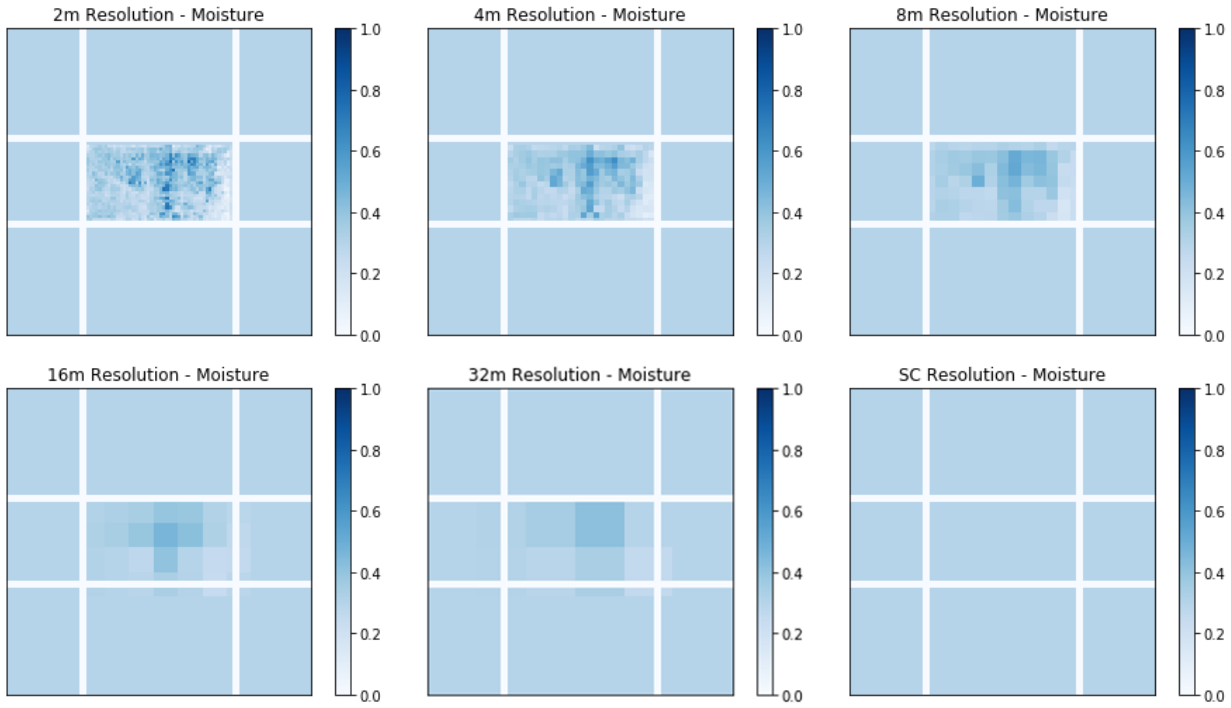

Results and Discussion

A. Surface fuels from Terrestrial Laser Scanning

Rowell (2017) demonstrated strong relationships between occupied volume and fuel mass measured by two-dimensional clip plots explaining 84% of the variability of surface fuel mass in frequently burned longleaf forested sites and 71% of the variability for non-forested grass and shrub matrices found on and near the EAFB B-70 range. This method was replicated for the Pebble Hill Plantation dataset, where occupied volume explained 44% of the variability of fuel mass in the surface fuelbed (**Fig. 13A**). This approach did not adequately match measured fuel mass at the wiregrass landscape and shrub dominated units. New methods for developing 3D fuel inputs from TLS were developed as a result, specifically a novel adaptation of Andersen's porosity metric from at a $10cm^3$ voxel scale and a mesh wrapping protocol that derives surface area of elements within each $10cm^3$ voxel cells. The models developed represent the bulk density of fuels (grams cm^3), where regression model coefficients and errors are described in **Table 3**. TLS derived maximum porosity (0-10cm and 10-20 cm strata) for a multiple linear regression explained 89% of the variability of the 0-10cm strata fuel bulk density (**Fig. 13B**) that accounts for the largest proportion of fuel mass in the surface fuelbed of frequently burned southern pine forests (Rowell et al. 2016). Mesh derived surface area for fuel strata above 10 cm in height performed well as a predictor of mass, where the model explained 69% of the variability of surface fuel mass in grass\forb dominated sites (**Fig. 13C**) and 52% of the variability in shrub dominated sites (**Fig. 13D**).

From the outset of this project, the expectation that studies conducted at EAFB as part of the RxCADRE experiments would be transposable to other landscapes in the southeastern United States. The initial comparisons with both the TLS and the 3D voxel sampling protocol derived occupied volume demonstrated (**Fig. 13E**) an underestimation of mass as compared to occupied volume which we attribute to two possible reasons: 1) a higher proportion of downed woody debris due to higher overstory stocking densities and 2) the longer fire interval at Pebble hill. The use of the porosity metric appears to improve estimates of mass, even when coarse woody material is

Figure 13. Occupied volume based predictions of bulk density from 3D clip plots (A) and TLS data (B). Bulk density estimates from the porosity multiple linear model (C), bulk density estimates from surface area of meshes for grass\forb (D) and shrub (E) sites.

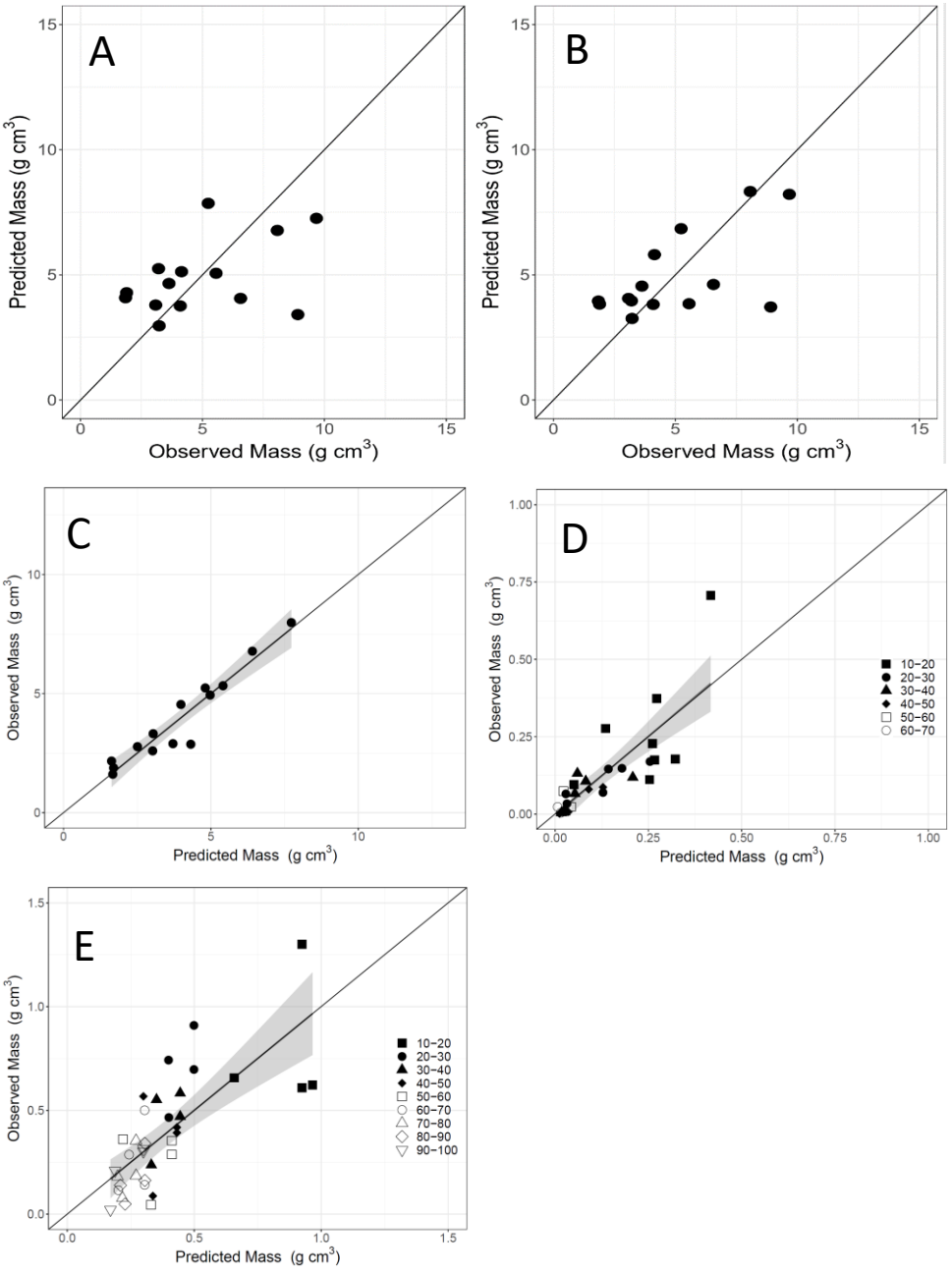

present, which represents an advancement in the science. The implications of re-evaluating the way we predict fuels using TLS data demonstrated value for both SERDP project RC-19-1329 and RC-19-1064. The approach detailed as part of this project has generated what we believe is a robust and replicable approach that not only improves upon the TLS research documented in Rowell (2017) and SERDP project RC-2243. Additionally, we report fuel mass as bulk density, which is the direct metric used in both HIGRAD/FIRETEC and QUIC-fire.

Table 3. Linear regression model coefficients predicting pre-fire fuel mass from porosity, surface area, and a combined model integrating the two estimates.

Predictor	Estimate	Std. Error	*t*-value	Pr(>|t|)	Significance
All 0-10 cm Biomass					
(Intercept)	457.8	33.5	13.65	3.1e-08	***
Porosity 0-10	-213.6	55.0	-3.89	0.00254	**
Porosity 10-20	-196.2	40.5	-4.85	0.00051	***
All Strata Biomass (Above 10cm)					
(Intercept)	0.718	1.566	0.46	0.65	
Surface Area	1.353	0.203	6.68	3.9e-09	***
Total Biomass (Combined Model)					
(Intercept)	38.765	16.446	2.35	0.0362	*
Combined Predictions	0.740	0.066	11.174	1.07e-07	***

Statistical significance for *p*-value: 0 '***' 0.001 '**' 0.01 '*' 0.05 '.' 0.1 ' ' 1

B. Surface and Crown Fuels from Airborne Laser Scanning

To aggregate fuels from the fine-grain TLS estimates of fuels we utilized the TLS data as training data for multiple linear regression after Hudak *et al.* (2016). In the before mentioned study, a model that The goal of this was to test if increasing the sample size of the selected a 3m radius area around each 1m x 1m plot were reduced to a series of statistical metrics to produce an optimized multiple linear regression to predict surface fuel mass. These metrics are described in Hudak *et al.* (2016) and the model using nine metrics explained 44% of the variability of fuel mass. This approach replicated by comparing occupied volume based models developed by comparing TLS data with the same two dimensional clip plots at Eglin Air Force Base (Rowell 2017) with prediction improvements by 30%.

Though the results of the surface fuels reported here are previously reported in Rowell (2017) and O'Brien (2017), this project marks the first use of the hierarchical sampling framework described as part of the RC-19-1064 proposal. The integration of richer remotely sensed fine-scale data as the source of training for increasingly coarser data. This has broader implications in regard to the information theory results presented in the fire behavior modeling portion of the study. We hypothesize that the finer starting grain of the TLS estimates of fuel mass and fuel type classification carry more information as resolution coarsens, suggesting that there should be investments to carry the diversity of fine-scale information to the initial coarse scales of ALS-derived surface fuel mass and type.

C. Simulated 3D Fuels

The 3D modeling of a pine needle litter layer is certainly feasible using current 3D modeling software. Detailed height maps (**Fig. 14)** can be generated in minutes, along with mass (**Fig. 15**), voxelized SAV (**Fig. 16**), and porosity (**Fig. 17**). In regards to fuel heterogeneity, even using a random uniform distribution to seed the needles in space and orientation, the rigid collision algorithm allowed for some variability to be added to the simulated litter fuelbed. This is equally compelling, as all the needle objects in the simulation are identical. Though we did not directly compare synthetic fuel heights against measured fuelbed metrics for this study, Rowell et al (2016) demonstrated that near identical object types in a Blender environment yielded Pearson correlations ranging from 0.75 to 0.94 when comparing simulated fuels with measured fuelbed height. In this same study, needle fuel mass calculated as a function of the surface area of each object demonstrated high correlation (r=0.86) between simulated needle and dry weight fuel mass.

SAV is an important fuel metric in CFD fire behavior modeling as this metric is associated with shape parameters (disk or cylinder) and is inversely proportional to the thickness of characterized fuel particles (Morvan and Lamorlette, 2014). Experimental observation fire demonstrate that fuels with a length scale less than 6mm account for 90% of the consumption in the flaming zone (Morvan and Dupuy, 2004). In CFD models generic SAV values are represented for large relatively homogenous surface fuel beds. SAV describes the receptivity of a particle to exogenous heat and moisture as a proxy of potential combustion (Marino et al. 2012). Using spatially explicit and highly resolved representations of SAV through simulation (**Fig. 18**) provides descriptions of SAV distributions vertically through the fuelbed. in this manner distributions for voxelized SAV and mass could be made allowing for possibly more sophisticated subgrid creeping fire-spread models. 3D modeling of this sort allows for a fuel bed to be probed without disturbance and whatever resolution desired. This methodology could be used to supply better parameterizations to high fidelity fire spread models. Ultimately one could use 3D models for other litter objects, build complex synthetic litter beds, then determine distribution parameters based off species percentages. Soft body interactions are needed to properly model the collection of litter fuels in shrubbery and other mid story fuels as well as the compression of needles under their own weight. Moving to another 3D modeling code such as Chrono, which is better parallelized and has more control in collision parameters, would be almost necessary to build more real-world fuel beds.

Figure 14. Height maps of the needle accumulation for 1000, 5000, 10000, and 15000 needles.

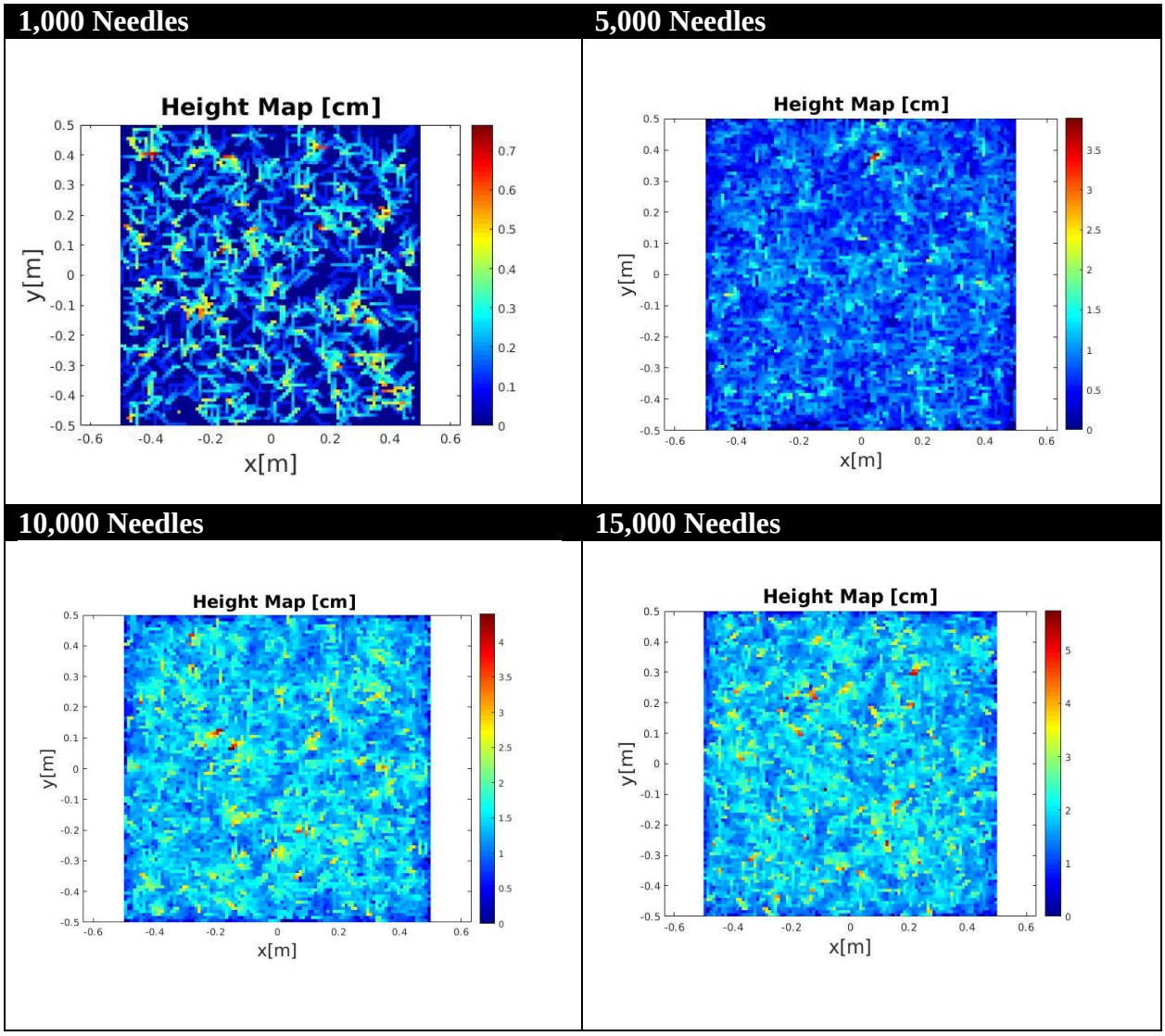

Figure 15. Plots showing the effect of coarsening on fuel heterogeneity for the needle litter from 15 thousand needles. Vertically integrated fuel mass per cell is plotted. Heterogeneity is diminished once cell sizes are larger than L.

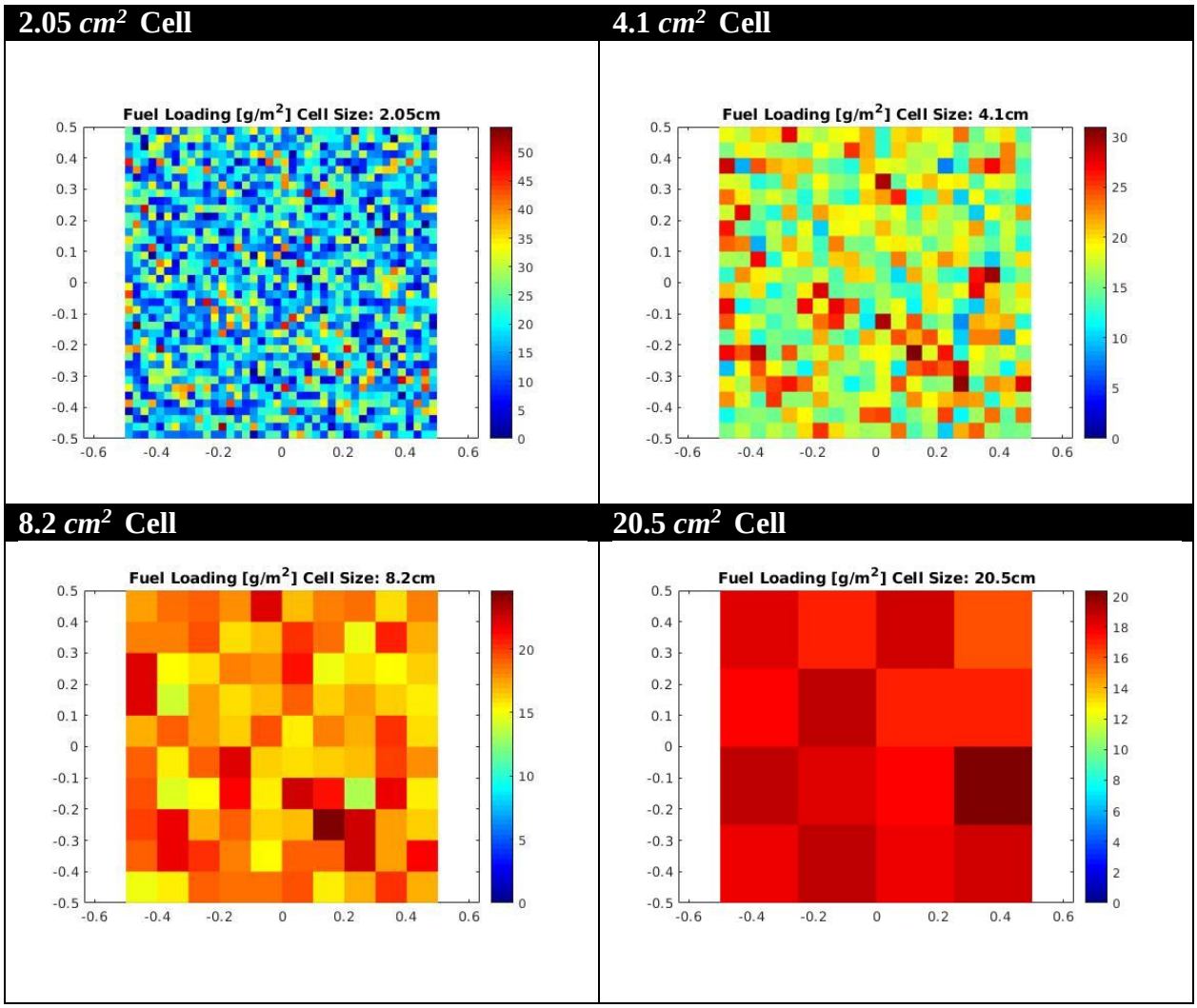

Figure 16. Plot showing voxel-averaged SAV from the 5,000 needle case. SAV is averaged across *y* position for the mid height value of the each layer (zmid) and shaded with the standard deviation. This figure shows that averaged SAV decreases with height from the floor suggesting that needles are packed closer together near the ground.

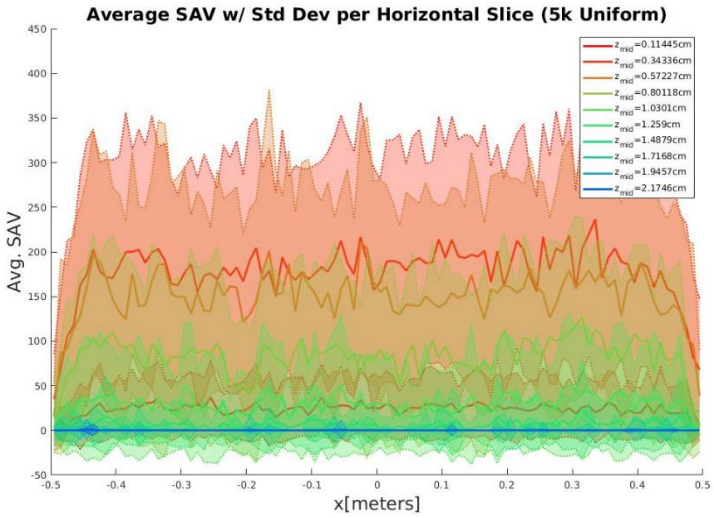

Figure 17. Histograms of the voxelized SAV for the 10k and 15k needle stacks. A similar shape is seen in both histograms but the higher needle count shows a broader distribution. This further supports the idea that needles are compacting together with higher needle counts, raising the mean SAV of the litter.

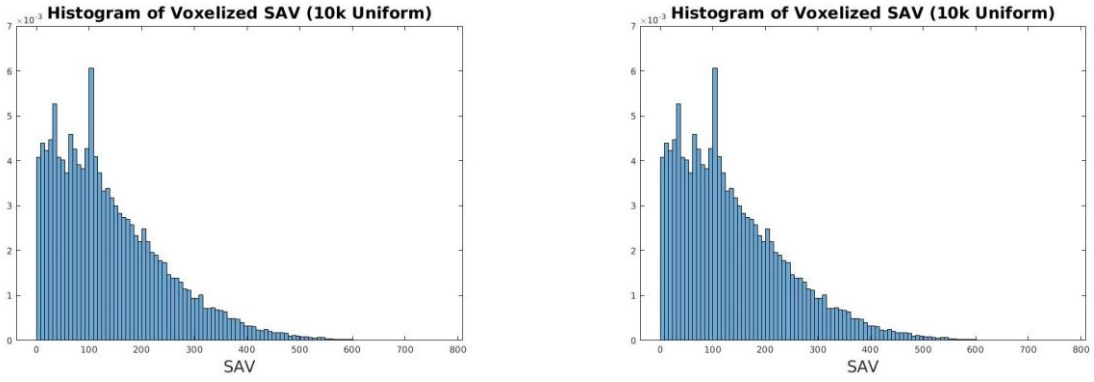

Figure 18. Histograms of the voxelized porosities for the 10k and 15k needle stacks. No significant difference is seen between the two histograms which suggests the higher SAV seen from increased needle count may just be a statistical effect. In other words, higher needle counts increase the chance of a falling needle filling an opening in the litter stack but does not mean a change in litter structure after a certain point.

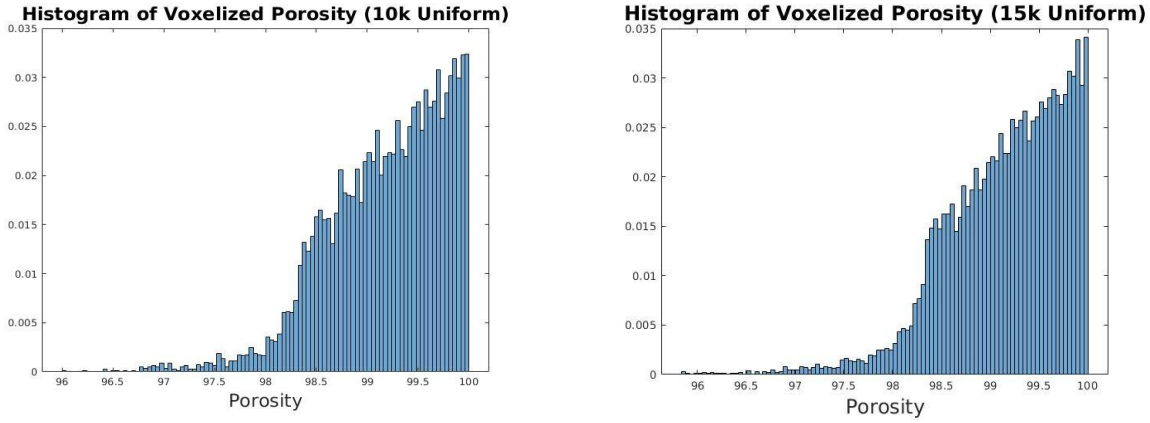

D. Ensemble QUIC-Fire behavior simulations small domain

A total of 2700 runs were performed using a laptop with 8 cores requiring almost 72 hours to run, demonstrating the relative efficiency of the QUIC-fire model. For each combination of environmental condition and resolution level, 50 runs were done for the initial Pebble Hill simulation. Fire behavior results showed distinct variation between environmental conditions and fuel resolution scales, with moisture level conditions having the least influence, and resolution scale having the highest (**Fig 19**).

Within-run variability was highly sensitive to all three main input variables: moisture level, wind speed, and level of resolution, with low levels of moisture, large scale of resolution and high wind speeds leading to highly variable behavior. Both burned area at end time (**Fig 19a**), and when looking at the max rate of growth (**Fig 19b**). Note that in these plots, single characteristic runs have a scale of resolution of 64m. For the burned area, at low wind speeds, the mean does not change drastically going from high to low resolution, but the variance does increase. Moderate and high wind speed conditions show significant changes on the mean and variance for burned area, with high resolution showing lower variance and higher burned area. Higher wind conditions show expectedly higher burned area, but also show much higher difference in the means depending on the resolution than in the low wind condition. These are also accompanied with a much higher variance than in high resolution conditions. Large levels of variation are expected in high wind conditions since there is larger uncertainty where the fire could spread. Large mean differences for different resolution levels on high wind speed cases was an unexpected result, since the expectations were that the fire behavior model would be more sensitive to resolution levels at marginal levels of fire behavior (i.e. low wind, high moisture conditions). Another unexpected result was a different fire behavior being observed at moderate levels of resolution, in particular

Figure 19: Ensemble run results for classic fire behavior metrics. Ensemble run results for a) burned area (m2) at simulation end time (t=400 s), b) max rate of growth (m2/s) and c) max rate of spread (m/s). Error bars are calculated by using the 90th percentile.

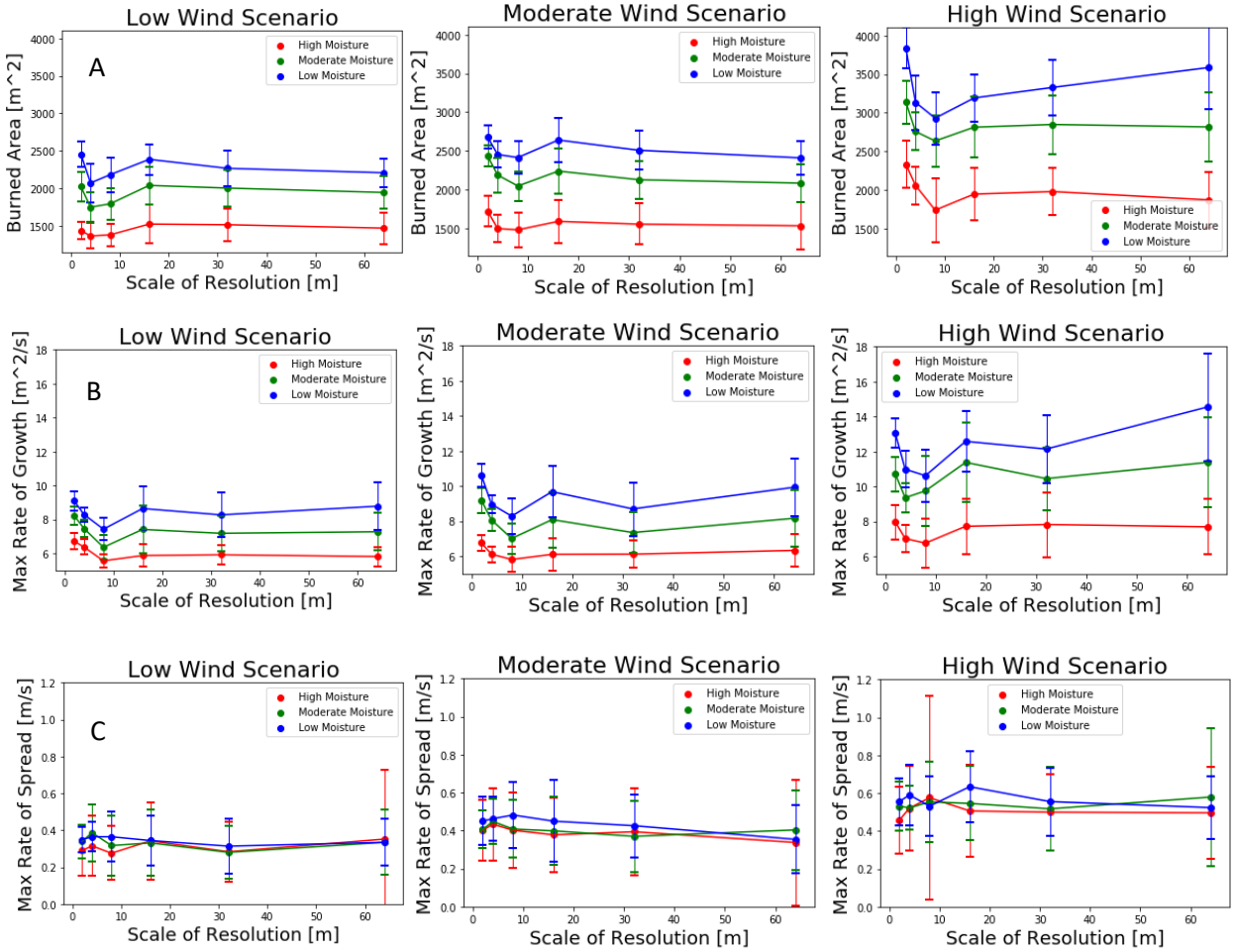

the 8m run, which showed higher variance for multiple metrics and a large dip for burned area over both low and high resolution.

The maximum rate of growth provides some clarity. In low moisture conditions, the mean is not significantly different for different resolution levels, but the variance is significantly higher. For all moisture and wind conditions, small resolution scale led to much lower variance. In high wind conditions, all moisture conditions have these same characteristics. Coupling the large difference in burned area for high wind conditions with a relatively similar max rate of growth indicates that low levels of resolution have much flashier fires, with large amounts of growth coming on bursts of intense fire behavior, while high levels of resolution tend to have much more stable predictable fire behavior. This is a similarly surprising behavior since lower levels of resolutions are essentially homogeneous grass, where we don't expect high levels of variance, but rather a constant burning fire. The same change in behavior for the 8m run is also visible in the max rate of growth with a large dip being present at that scale. An example of the min, median, and max burned density scenarios for the high wind, low resolution, low moisture condition burns are

shown in Figure 20 and comparisons of these same conditions over all resolutions is shown in Figure 21.

Two of the proposed metrics were meant to capture behavior that was more sporadic and relied on flashing fire over a constant growth. Reduced area, and the ratio between rate of spread and bulk rate of spread were calculated for each run. These new metrics are hard to interpret given the small effect of the input variables on the metrics, coupled with a large variance associated with several environmental conditions.

The reduced area should be lower for fragmented fire and should be higher for a constant spreading fire in all directions under a low wind (**Fig. 22**) . Flashing fire would show up as a dip in that curve. A sharp increase for the reduced area when moving from 2m to 4m to 8m resolution was the only common trait across all environmental conditions and it's likely related to the max rate of growth showing a dip for those same conditions as well. Since the fire was less prone to large bursts of fire behavior, it was likely a marginal fire. Variance for this variable was markedly higher for high moisture conditions, where highly fragmented fires were the norm and increasingly marginal fire behavior was expected.

Figure 20: Fuel consumption variety at simulation end time. Fuel density at simulation end time for the a) min, b) median, and c) max of burned case scenario for a low resolution, high wind, low moisture run.

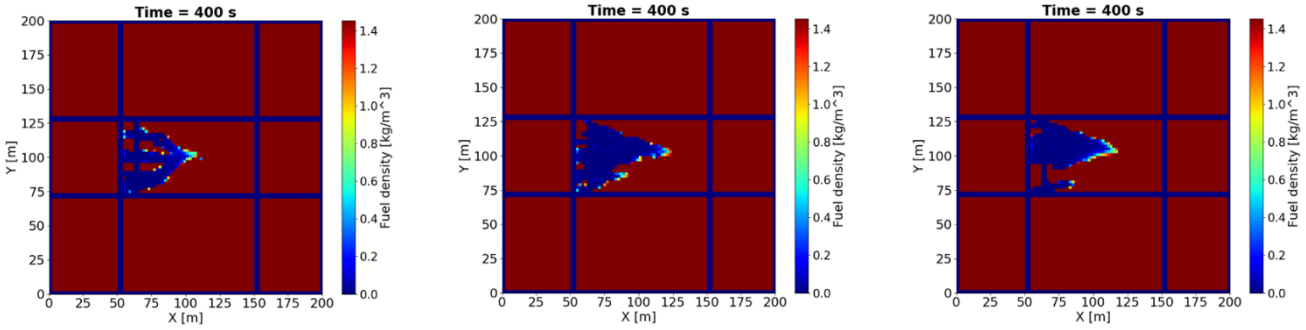

Figure 21: Fire behavior at different levels of fuel resolution. Fuel density at the surface level for a low wind / low moisture condition for a) 2m, b) 4m, c) 8m, d) 16m, e) 32m, and f) single characteristic.

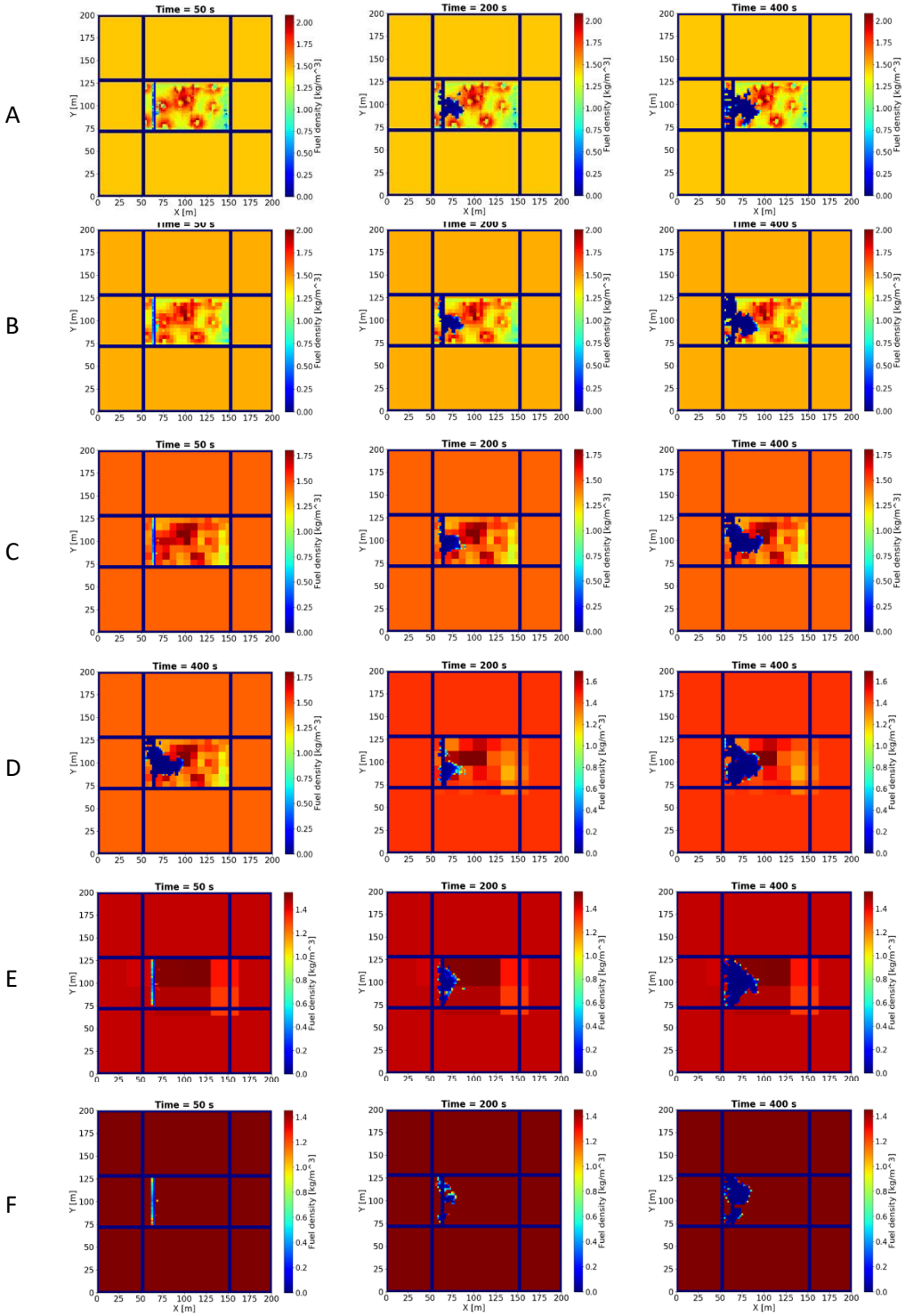

Figure 22: Ensemble run results for the reduced area. Error bars are calculated by using the 90th percentile from the ensemble runs. X-axis represents the scale at which the fuels were aggregated prior to the run starting.

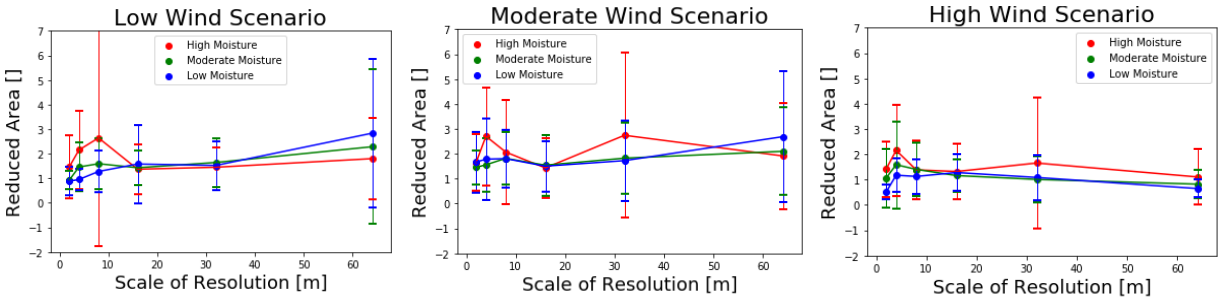

Figure 21: Ensemble run results for the max RoS/BRoS for all conditions. Error bars are calculated by using the 90th percentile from the ensemble runs. X-axis represents the scale at which the fuels were aggregated prior to the run starting.

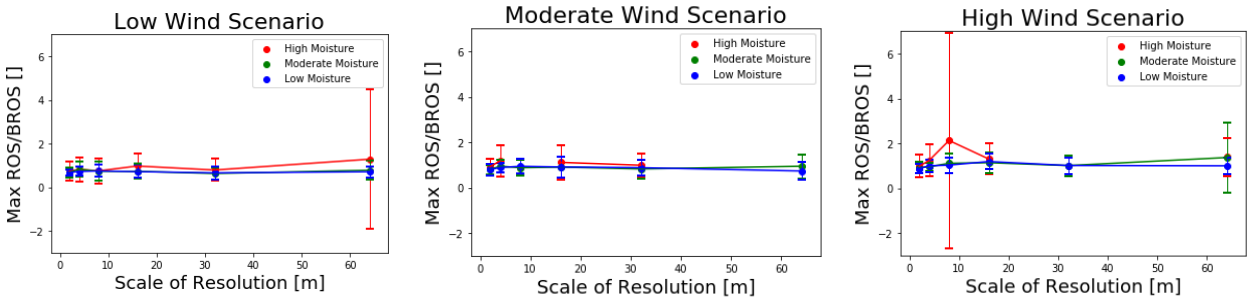

Max ROS/BROS is meant to represent how much of the fire spread is going in the forward as opposed to the lateral and backward spread (**Fig. 23**). These was hard to interpret but varied mostly with wind speed, with moisture content and resolution level having little to no effect on it. Runs where it did vary, as with moderate wind speeds had large variance associated with it which made it harder to interpret. This metric was found insufficient and provided little to no information on fire behavior, even for cases where high levels of difference were expected.

An important metric that measured fire behavior spread was the normalized canopy consumption. Shown in Figure 24, canopy consumption was much higher for low levels of resolution, where the scales of aggregation were large enough that averaging canopy fuels led to a continuous layer of low-density fuel. Due to the nature of aggregating at every vertical layer, the high-resolution runs had a much lower canopy cover, and as such had a higher wind speed felt at the surface. It also meant that sustaining a crown fire was much more accessible for low resolution runs, since once a single cell exhibited torching, the low fuel density in the contiguous cells led to a relatively small amounts of moisture needed to be removed in order to ignite that next cell, and since there were no significant gaps in the crown, the crown fire could sustain itself with little help from a surface fire. This led to high normalized canopy consumption, while low resolutions have low levels even if they are igniting canopies.

The uncertainty created by different canopy covers and the effects it might as possible explanations for differences inspired a set of similar runs where the aggregation occurred only in the surface levels. This is justified since for the methodology presented here, the information required for surface and canopy layers come from different components of instrumentation. Due to time limitations, ensemble runs were not possible, but results for a single run for each permutation of environmental condition and resolution level for burned area, max area growth, and normalized canopy consumption are shown in Figure 25. The high variability seen on the runs where all vertical layers are horizontally aggregated indicate that these results are only preliminary but are nonetheless important to understand the causes between the large differences in resolution levels through environmental conditions.

Burned area and max rate of growth are much more sensitive to wind conditions, with low wind conditions being markedly lower for a surface level averaging than for a full domain averaging, but higher wind speed conditions having generally higher burned area. This is particularly true for larger scales of resolution, where a full canopy cover could slow down the winds felt at the surface considerably, leading to much smaller burned areas. A larger parameter sweep for wind speeds would be interesting since there is a large shift in behavior from moderate to high wind conditions. The max rate of growth across the board is much lower than for the full domain averaging indicating much more constant heading fires as opposed to the flashy fires that characterized the low resolution runs in moderate and high wind conditions. Normalized canopy consumption is expectedly down and has leveled off for runs making it wholly dependent on fuel moisture and wind speed, and not to the level of resolution. This is important to properly interpret probability of torching and existence of crown fires from fire behavior model runs. It's important to notice that low wind conditions have higher normalized canopy consumption (**Fig. 24**), but it makes sense since the surface consumption would be much lower for these runs, making the first torching trees have a greater impact on the metric since it's not weighed down as much by the rest of the surface fuel consumption. Figure 26 shows the fuel density for surface and crown fuel for two runs at 2m shows the fuel density for surface and crown fuel for two runs at 2m and 64m aggregation levels. Note that while torching does occur, a crown fire cannot be sustained on these conditions.

Figure 24: Ensemble run results for the normalized canopy consumption. Error bars are calculated by using the 90th percentile from the ensemble runs. X-axis represents the scale at which the fuels were aggregated prior to the run starting.

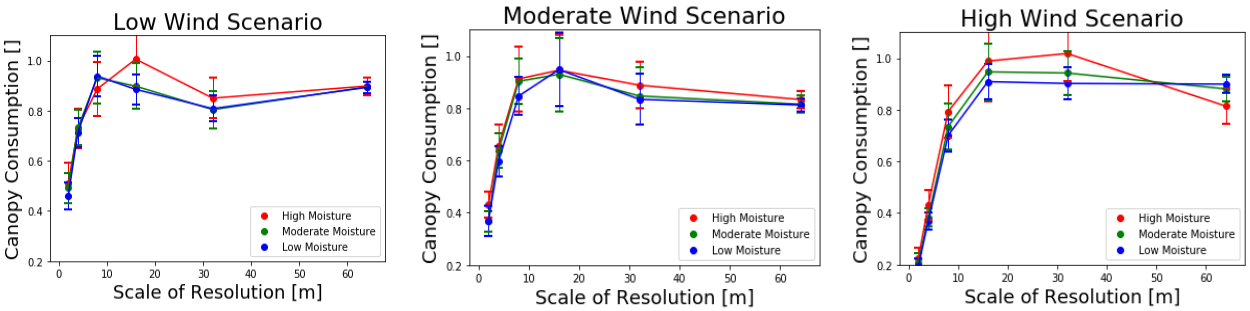

Figure 25. Results for surface fuel aggregation as opposed to aggregation of all vertical layers. Ensemble run results for a) burned area (m2) at simulation end time (t=400 s), b) max rate of growth (m2/s) and c) normalized canopy consumption () for all runs. Error bars are calculated by using the 90th percentile from the ensemble runs. In pink, cyan and lime green are shown the single run results for runs averaging only the surface fuels.

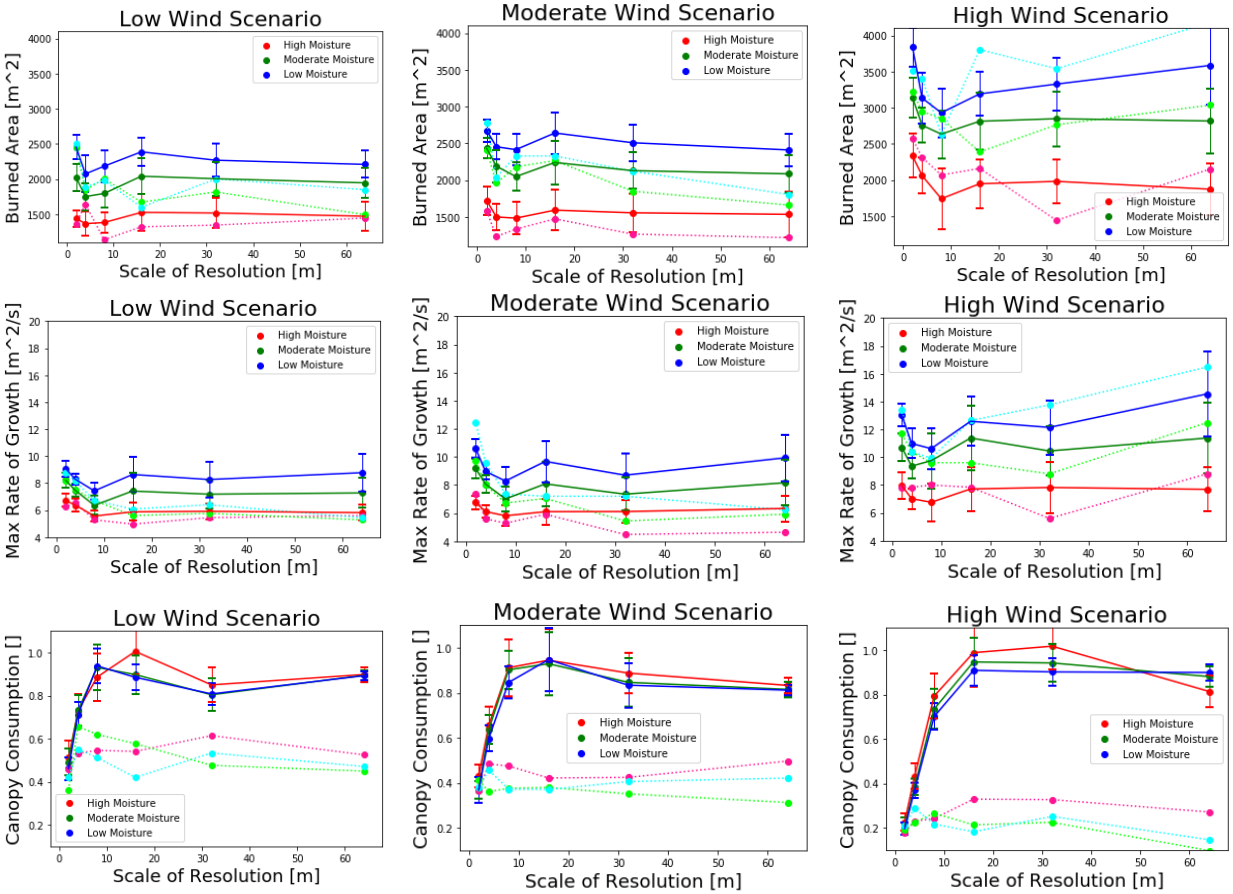

Figure 26. Surface and canopy consumption for a surface fuel aggregation. Surface fuel density at simulation end time for a) a 2m resolution run, c) a single characteristic run, and fraction canopy fuel remaining for b) 2m resolution run, d) single characteristic run.

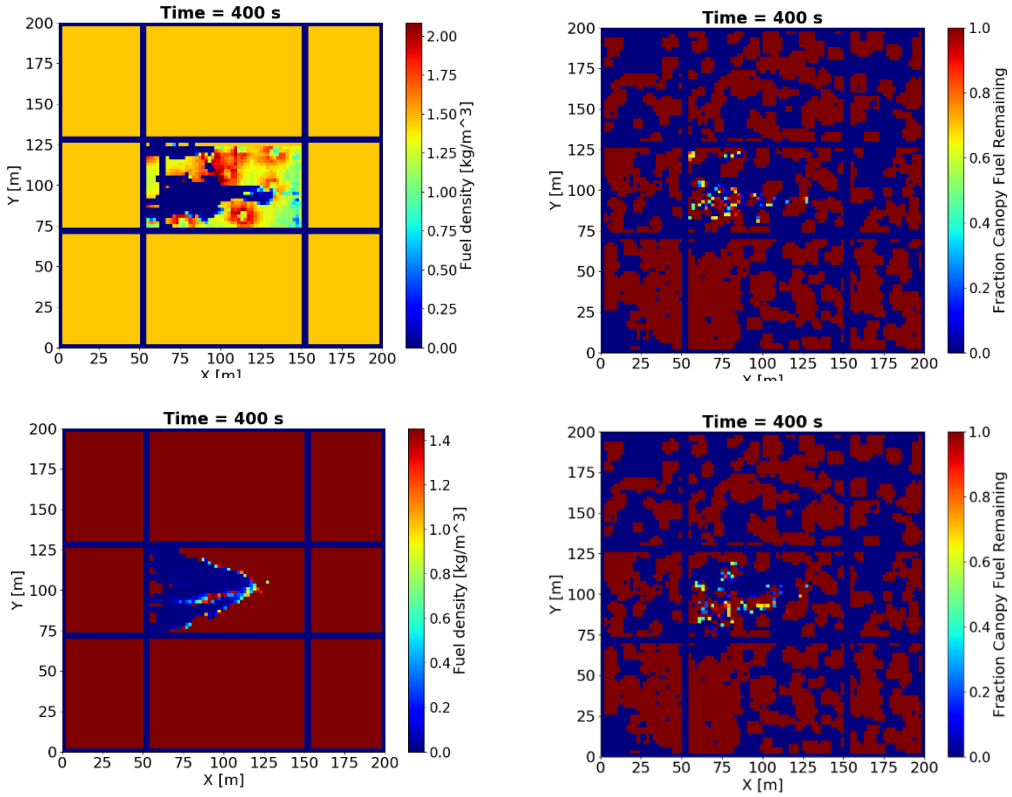

We can also look at the effect of adding more information into the system and the effect it has on fire behavior. We employed Shannon's diversity index to assess information loss over coarsening of scales. Figure 27 shows how the diversity index changes for different scales of resolution for different categorization schemes. Two important facets to note are that the information change for fuel species is not significant, and information loss for the relevant categories of grass, shrub and represent a slow decay until the single characterization plot (64m resolution). Evaluating at these categories more closely, the litter category starts off at a low percentage and is quickly absorbed into the grass category. Due to the inherent structure in the system where shrubs had clumped together, not much more information is added by going from 16m down to 2m resolution. The fuel density categories and information loss between scales change drastically across different scales of resolution. The diversity index for both the 32m run are significantly lower than those for high resolution, with 32m runs being concentrated on two contiguous categories. The fuel density is then shown not to vary too highly at these scales. However, there were large differences when going from 16-32m, and from 8-4m in resolution, which indicate that while the fuel height might not change drastically at these scales, the fuel density does. Also, important to note is that for the fuel species categorization, the diversity index increased for a 32m resolution compared to 16m resolution. This is likely due to the low number of categories (at that point, just grass and shrub). This led to the creation of another fuel moisture

category going on 5% percentiles from 0 to 1, from dead fuel moisture to live fuel moisture. This is shown in green in figure 27A, and tracked through different moisture conditions in figure 27B. This shows a similar trajectory to the initial fuel moisture categorization in terms of species, but also does not show the aberration from having too few categories. There was not much differentiation seen from the different moisture conditions, since the averaging occurs between relatively low moistures of dead fuel compared to live fuel regardless of the low moderate or high moisture condition.

Figure 27. Shannon diversity index for different categorization schemes

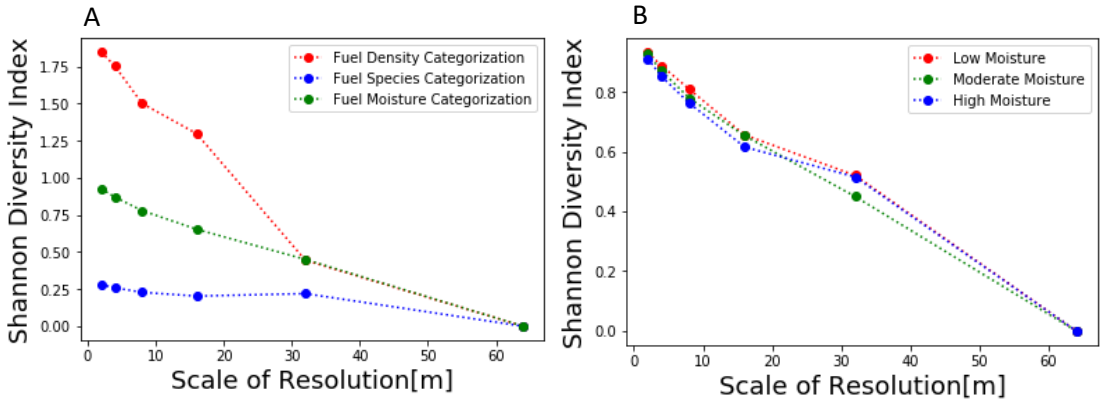

Using the diversity index on the output (**Fig**. **28**) as a function of the detailed fuel moisture input diversity index. Since different levels of resolution there are only two categories for the output diversity index, small changes from similar conditions aren't as drastic as the effects coming from different levels of moisture or wind speeds. Another issue of only having two categories, is that it's essentially undistinguishable to have a run where almost no fuel was burnt and almost all the fuel was burnt. Since the categories are weighed the same, these would appear completely the same, even for different levels of resolution. This can be seen when looking at the drastic change in behavior from low and moderate winds, to high wind scenario, where the high moisture content run goes from being the one with the lowest diversity index to the highest. This is because the low moisture run burns almost the entire domain, leaving little to no change and appearing as having lower diversity.

Figure 28. Results of diversity index as output variable. Shannon diversity index for fuel density at simulation end time as a function of the detailed fuel moisture diversity index.

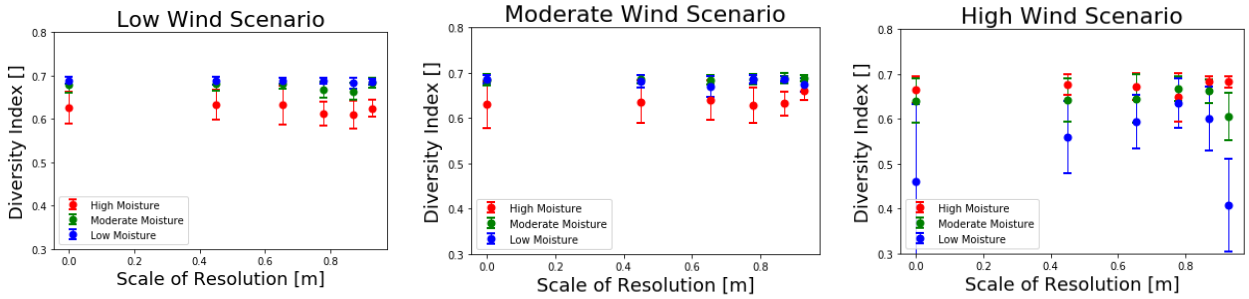

Statistical results show the complex interactions among environmental variables. All interactions were significant for burned area, all but one (interaction of resolution scale and moisture) were significant for max rate of growth but only the main effect of wind speed was significant for max rate of spread. Moisture level was the most significant predictor for burned area, since it modifies the amount of available flashy fuels within the computational domain. The interactions within variables for the burned area are all interesting. Resolution scale has a negative impact on burnt area but positive interactions with both moisture and wind speed, meaning that at higher levels of moisture and higher wind speed conditions, the resolution scale's effect would be more pronounced. Max rate of growth expectedly depended pretty evenly on wind speed and moisture content, with scale of resolution being the least important main variable. The most surprising result is that the max rate of spread is only dependent on the wind speed. While this is an assumption commonly used in decision making tools, fire behavior metrics have usually moved past that simple dichotomy. Note that this does not mean that the fire will move the same distance over the simulation runtime, since this is just the max rate of spread.

The interaction between wind speed and moisture with resolution level was interesting and there was high likelihood that it was reflecting the dip for burned area for the 8m run. When observing the moisture levels of the fuels where the fireline is initiated moderate levels of resolution have a large number of cells being ignited near large high moisture blocks, which would inhibit the initial fire growth and have large effects for burned area downstream. At high levels of resolution, there are enough low moisture cells scattered around that the initial ignition can reliably find low moisture cells to ignite quickly and effectively. At low levels of resolution, the averaging over a larger number of cells lowers the moisture levels near the ignition lines enough to enable a strong head fire within those areas. To test out the effect that the position of the initial fire line could have, a series of ensemble runs were performed where the initial fire line was shifted 5m to the left and 5m to the right.

Figure 29. Ensemble run results for maximal downwind spread (m). Error bars are calculated by using the 90th percentile from the ensemble runs. X-axis represents the scale at which the fuels were aggregated prior to the run starting.

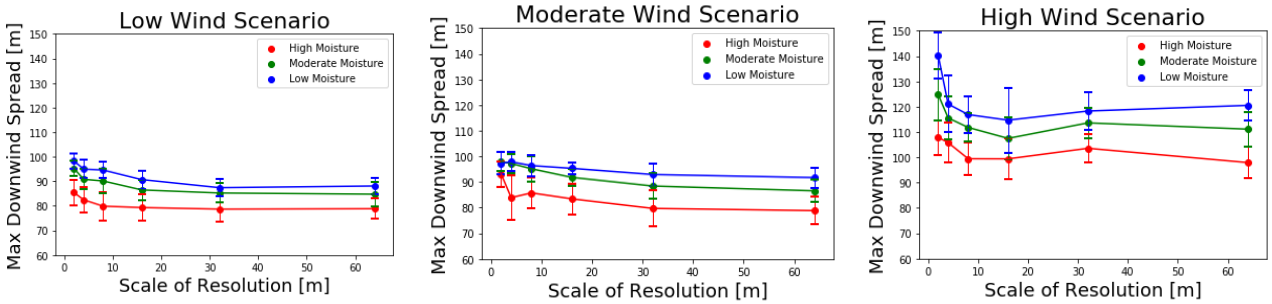

To better elucidate the how changes in the resolution of the fuel information influence the fire simulation, the moisture content and wind speed cases were combined into a single data set using the Fosberg fire weather index (Fosberg 1978). The Fosberg fire weather index is a non-linear filter of meteorological data designed to provide a linear relationship between the combined weather inputs and wildland fire behavior by following the same principles as the flame length model of Byram (1959).

Figure 30. Percent change in Shannon diversity index as a function of the scale of resolution of the fuel information for the 4 highest intensity fires from Table 4.

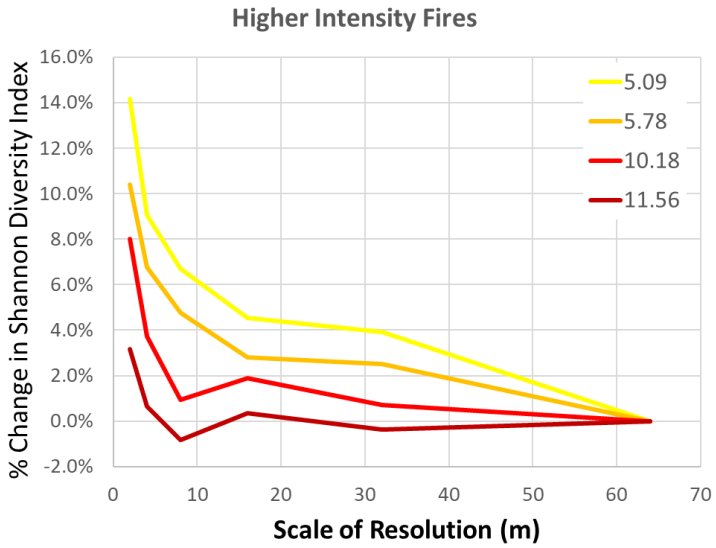

Figure 30 shows how the information content as measured by the Shannon Diversity Index of the amount of energy released to the atmosphere changes as the resolution of the fuels change for the four highest values of the Fosberg fire weather index shown in Table 4. For the highest intensity fire little information is gained as the level of detail in the fuel input increased, but as intensity decreased more information from the fuels layer became evident in the fire's simulated behavior. However, this trend did not continue for the lowest intensity fires from Table 4 (Figure 31). Instead the lower intensity fires exhibited similar information gains without a clear intensity-based pattern.

Table 4. Fosberg Fire Weather Index values as a function of fuel moisture content and wind speed.

		Wind Speed (m s^{-1})		
		3	6	12
% Moisture Content	4	2.89	5.78	11.56
	8	2.54	5.09	10.18
	16	1.07	2.13	4.26

We hypothesize that this change in response is tied to the model's inability to resolve the processes important for maintaining the fire at these low intensities. An example of one of these key processes is the generation of turbulence by buoyant motions associated with the flaming front. As the depth of the flaming front shrinks below the grid size of the fire model, the buoyant updrafts become poorly resolved and thus remove a source of turbulence that helps maintain the combustion

process. A second piece of this hypothesis is that the information gain we do see for these low intensity fires is tied to changes in the influence of vegetation drag resulting from increased detail in the fuels. The vegetative drag provides a source of turbulence that while not as strong as that of the fire's buoyancy, is capable of maintaining the combustion process to some degree. As many prescribed fires tend to feature only limited amounts of head fire with much more of the spread occurring as a mixture of flanking and backing spread, how fire behavior models perform under these lower intensity conditions will be a determining factor in their ability to assist land managers in the prescribed fire planning process.

Figure 31. Percent change in Shannon diversity index as a function of the scale of resolution of the fuel information for the 4 lowest intensity fires from Table 4.

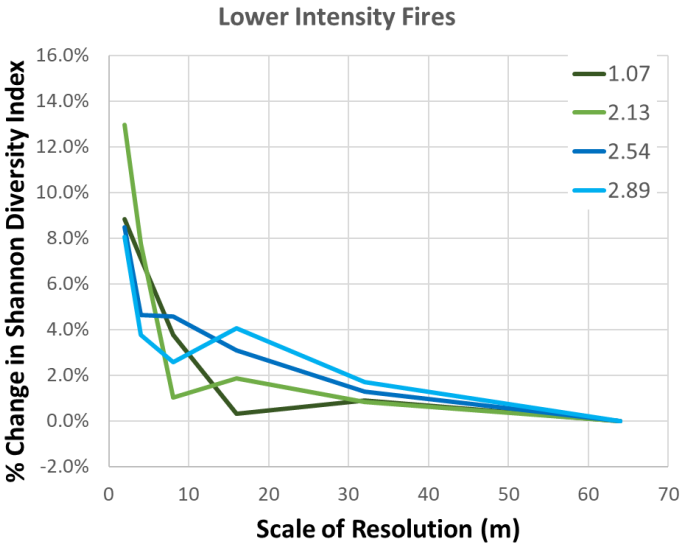

Figure 32. Shannon diversity index for different categorization schemes (A) and categorization of available fuel moisture (B).

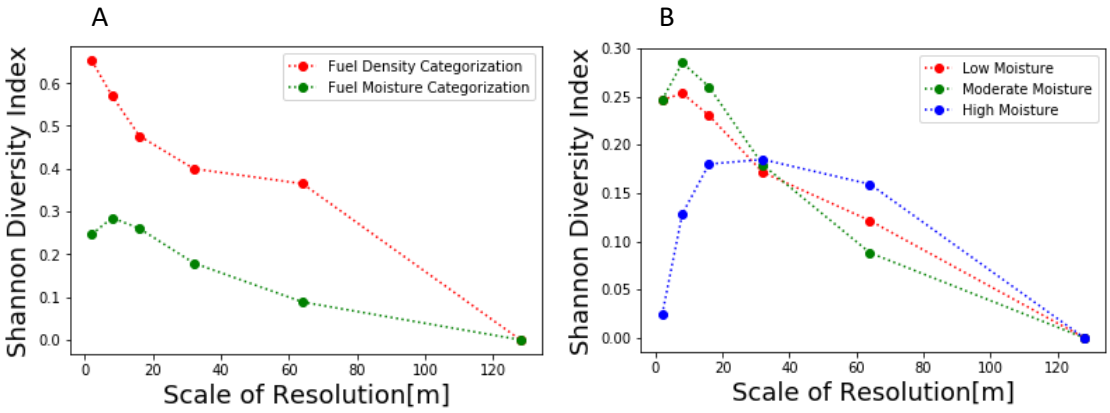

E. Ensemble QUIC-Fire behavior simulations large domain

Using the diversity index for fuel density and fuel moisture categories on as a function of scale, two key trends are apparent. As scale increases the heterogeneity or information associated with

the fuel density responds with an expected degradation (**Fig. 30**). Of interest is the response from the fuel moisture categorization which increases in diversity as scale coarsens from 2 to 4m voxel domains. This result corresponds with the moderate and high moisture scenarios, where gains in heterogeneity are demonstrated at peak of 8m voxel scale in the moderate moisture scenario and 16m voxel domains for the high moisture scenarios. The coarser scale of the EAFB input data and larger modeling domain (**Fig. 31)** confound the fuel moisture responses in the diversity index when compared with the Pebble Hill simulations. The range of values from the diversity index are reduced versus the values from the fine-scale fuel metrics described in the Pebble Hill data set suggesting that there is a reduction in heterogeneity by estimating the fuel metrics at a $25m^2$ grainsize. This finding has implications that alternative methods of aggregation and estimation to landscape scales may be necessary to carry inherent variability to coarser scales.

Figure 33. The QUIC-fire simulations for the high moisture EAFB runs showing fuel density (A) and fuel moisture (B).

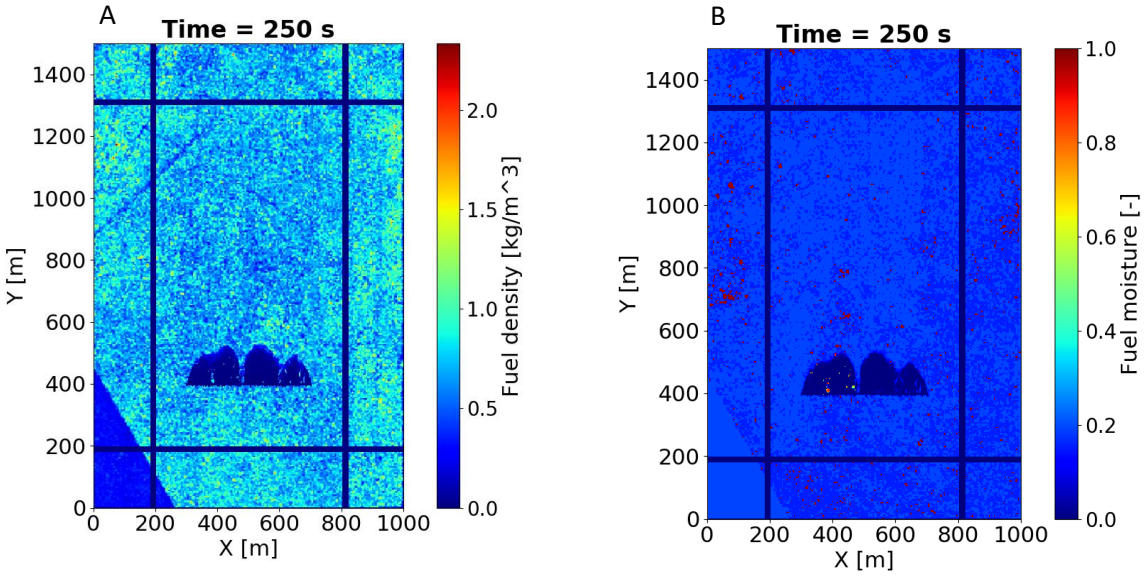

Conclusions and Implications for Future Research

The ability to address scaling in the domain of both full physics-based and hybrid quick solving CFD models is a link to understanding tradeoffs for speed versus accuracy that are essential to prescribed fire managers. The most fundamental input to inform scaling are the representation of fuels three-dimensionally.

Optimal input scale:

Our primary objective was to determine optimal scales for inputs that result in robust estimates of fire behavior important to fire managers on DoD lands. The results of this research suggest that

unsurprisingly fuels inputs are the primary driver of expected energy release when coupled with factors of fuel moisture and wind.

The resolution of these fuels provide the highest levels of information when aggregated from the finest scale, in this instance TLS-derived bulk density. These data encapsulate the best possible characterization and demonstrably lose information as a function of scale coarsening, but the cost of the loss of information in regards to fire intensity depends on the conditions of the fire. Under conditions favorable to rapid growth and high intensity, the role of input scale is less important as wind, buoyant motion, and resulting flaming depth. These conditions supersede the information of the fuels, suggesting that coarser scale data (8-20m voxels) are appropriate for fire that occurs under critical upper end thresholds. Under more marginal conditions the scale of fuels is a critical driver of fire growth and behavior as a function of drag and therefore the finest resolution data are necessitated for these types of prescribed fire simulations. The scales these types of fuels encompass are <1m to 2m voxel sizes and can be characterized in the subgrid processes of both HIGRAD\FIRETEC and QUIC-fire or other fine grain CFD models as the Wildland Fire Dynamics Simulator (WFDS). Between the contrast of both extremes, expectedly mid-range fire weather simulations would require inputs that fall within the 2-10m voxel domain for bulk density inputs accounting for drag effects and canopy interaction.

Fuel type specificity and moisture categories are also important factors that tie to the ability for bulk density to engage in combustion. With limited data regarding fuel type on the sites used in the simulation framework, we relied on a basic logic of three primary categories of litter, grass, and shrub. Coarsening of these variables led to limited information loss ostensibly due to the small categorical groupings. Whereas the fuel moisture categorization had twenty potential classes that encompassed both live and dead fuel moisture and produced a linear decay of information as scale coarsened.

Knowledge Gaps

To further explore this line of inquiry, we focused on the derivative products of both TLS and ALS data to parameterize our analysis of scale as a function of the diversity index. We did not include information about spatial neighborhood effects. Alitieri et al. (2017) describe ways to integrate spatial clustering and neighborhood metrics. The additive element of spatial-based elements may also effect the information being conveyed through fire behavior outputs that could prove to be equally informative in regards to both voxel scale and neighborhood influence. A missing element to all of these avenues is the comparative analysis of the range of the diversity index at each data and domain scale. The diversity of variability for the Pebble Hill site was higher than that of the EAFB site. In turn, we would hypothesize that the simulation outputs and the 3D voxel plots would exhibit higher diversity index values then the before mentioned data sets. Thus, identifying those linkages between data scales is an obvious aspect of future investment.

Future Research

Future research should include the facets discussed in this section, specific investments to understand these scaling effects have significant impacts on numerous funded research programs through SERDP. From this research we have identified a set of recommended future research themes, including;

Integration of an automated fuelbed simulator is the next step in the advancement of fuels characterization. A prototype environment that produces rational estimates of needle litter was produced as part of this project, but learning curve and adjustments to develop more automated and objective methods of simulation proved to require a more significant investment. These simulations integrate not only three-dimensional bulk density estimates, but other intrinsic fuel properties (SAV, porosity, fuel type) that would add dynamic inputs to support CFD modeling initiatives. The key advantage of this research direction is the ability to generate robust estimates of fuels without the expense of remotely measuring the site with TLS or ALS systems and directly linking the simulations with readily available data such as aerial imagery to populate fuelbeds. The direct benefit of using of using fuelbed simulated objects is the detailed accounting of all features in the fuelbed, where effects of occlusion and inability to segment laser data into tenable fuel categories is eliminated. Additionally, robust characterization of fuel characteristics would challenge existing assumptions within CFD models that already generalize fuels inputs to simplify combustion code embedded in the models. The products generated from the simulation space should also have a user design interface, where managers could easily assemble and arrange fuel objects to generate inputs to CFD models that could represent existing units, out of prescription units, or optimal condition units to test assumptions of prescribed fire simulations. We have termed this concept "FUELScraft", which could have direct linkages to three dimensional crown\tree simulation frameworks as STANDFIRE, and direct benefit to the 3D fuels characterization SERDP project (RC19-1064).

In this project the changes in information in regards to fire outputs as energy to the atmosphere assumed generalized ignition and wind patterns with changes in scale driven primarily by fuel inputs. Simulated fire behavior responded to the increased information in the fuels layer, however the pattern of response warrants further investigation. As fire intensity decreased, the response to added fuel information increased up to an apparent threshold. Further study should investigate this threshold behavior with multiple models and various subgrid parameterizations to ascertain whether this behavior is universal to CFD-based models and can the behavior be overcome through improved representation of subgrid processes or is higher model resolution the only recourse. Behavior of these lower intensity fires is critical for a range of prescribed fire applications. To better management prescribed fires, land managers need practical tools capable of simulating fire behavior across a range of conditions, both high and low intensities, and these tools subsequently need to provide appropriate input to fire effects models for evaluating fire objectives. Improving our understanding of the behavior of CFD-based models at these lower limits of fire intensities is critical for determining their near-term practicality as a tool for land managers.

Benefits

The results of this research benefits DoD fire managers by providing an expected range of scales that affect spread and intensity of simulated fire using a quick solving CFD model. This research also helps managers assess data needs that will better inform expected fire behavior that supports prescribed fire objectives across DoD and other federally managed lands, specifically in predicting fire for marginal burn prescriptions.

Literature Cited

Altieri L, Cocchi D, Roli G (2017) The use of spatial information in entropy measures. https://arxiv.org/abs/1703.06001

Anderson HE (1969) Heat transfer and spread. USDA Forest Service, intermountain Forest and Range Experiment Station, 29pp.

Byram GM (1959) Combustion of forest fuels. In 'Forest fire control and use'. (Ed. KP Davis) pp. 61-89. (McGraw Hill: New York).

Feng D, Tierney L. (2008) Computing and displaying isosurfaces in R. Journal of Statistical Software, 28, 1-24.

Fosberg MA (1978) Weather in wildland fire management: the fire weather index. Conference on Sierra Nevada Meteorology, pp. 1-4, June 19-21 Lake Tahoe CA.

Gallagher MR (2017) Monitoring fire effects in the New Jersey Pine Barrens with burn severity indices. Rutgers University-School of Graduate Studies.

Hawley CM, Loudermilk EL, Rowell EM, Pokswinski, S (2018) A novel approach to fuel biomass sampling for 3D fuel characterization. MethodsX, 5, 1597-1604.

Hiers JK, O'Brien JJ, Mitchell RJ, Grego JM, Loudermilk EL (2009). The wildland fuel cell concept: an approach to characterize fine-scale variation in fuels and fire in frequently burned longleaf pine forests. International Journal of Wildland Fire, 18, 315-325.

Hiers JK, O'Brien JJ, Varner JM, Butler BW, Dickinson M, Furman J, Gallagher M, Godwin D, Goodrick SL, Hood SM, Hudak A, Kobizar LN, Linn R,, Loudermilk EL, McCaffrey S, Robertson K, Rowell EM, Skowronski N, Watts AC, Yedinak KM (2020) Prescribed fire science: the case for a refined research agenda. Fire Ecology,16:11.

Hilton JE, Miller C, Sullivan AL, Rucinski C. (2015) Effects of spatial and temporal variation in environmental conditions on simulation of wildfire spread. Environmental Modelling & Software, 67:118-127. https://doi.org/10.1016/j.envsoft.2015.01.015

Hough WA, Albini FA (1978) Predicting fire behavior in palmetto-gallberry fuel complexes. Research Paper SE-RP-174.Asheville, NC: USDA-Forest Service, Southeastern Forest Experiment Station. 48 p.

Hudak A, Bright B, Pokswinski S, Loudermilk EL, O'Brien, JJ, Hornsby B., Klauberg C, Silva C. (2016). Mapping forest structure and composition from low density lidar for informed forest, fuel, and fire management across Eglin Air Force Base, Florida, USA. Canadian Journal of Remote Sensing, 42, 411-427.

Johnson E, Miyanishi K. (2001). Strengthening fire ecology's roots. In Forest Fires: Behavior and Ecological Effects, ed. E. Johnson and K. Miyanishi, 1-9.San Diego, CA: Forest Fires: Behavior and Ecological Effects https://doi.org/10.1016/B978-012386660-8/50003-9

Ladislav K (2003). Rigid Body Collision Response. 7th Central European Seminar on Computer Graphics.

Kuhn, M. (2013). Predictive Modeling with R and the caret Package.

Linn RR, Reisner J, Colman JJ, Wintercamp J (2002) Studying wildfire behavior using FIRETEC. International Journal of Wildland Fire, 11:4, 2223-246.

Linn RR, Cunningham P (2005) Numerical simulations of grass fires using a coupled atmosphere–fire model: basic fire behavior and dependence on wind speed. Journal of Geophysical Research: Atmospheres, 110.

Linn RR, Sieg CH, Hoffman CM, Wintercamp J, McMillin JD (2013) Modelling wind fields and fire propagation following bark beetle outbreaks in spatially-heterogeneous pinyon-juniper woodland fuel complexes. Agricultural and Forest Meteorology. 173: 139-153.

Linn RR, Goodrick S, Brambilla S, Brown MJ, Middleton RS, O'Brien JJ, Hiers JK (2020) QUIC-fire: a fast running simulation tool for prescribed fire planning. Environmental Modeling and Software, 125:104616.

Lorensen WE, Cline HE. (1987). Marching cubes: A high resolution 3D surface construction algorithm. In, ACM siggraph computer graphics (pp. 163-169): ACM.

Marino E, Hernando C, Madrigal J, Díez C, Guijarro M (2012) Fuel management effectiveness in a mixed heathland: a comparison of the effect of different treatment types on fire initiation risk. International Journal of Wildland Fire **21**, 969-979.

McCuller S. (2013). A dangerous servant and a fearful master: why Florida's prescribed fire statute should be amended. Florida Law Review 65: 587.

Mcgaughey, R. (2014). FUSION/LDV: Software for LiDAR data analysis and visualization - V3.10. USDA Forest Service.

Mitchell, RJ, Hiers JK, O'Brien J, Starr G. (2009). Ecological Forestry in the Southeast: Understanding the Ecology of Fuels. Journal of Forestry, 107, 391-397.

Morvan D, Dupuy JL (2004) Modeling of fire spread through a forest fuel bed using a multiphase formulation. Combustion and Flame, 127, 1981-1994

Morvan, D, Lamorlette A (2014) Impact of solid fuel particle size upon the propagation of a surface fire through a homogeneous vegetation layer. Fire Safety Science 11: 1326-1338. 10.3801/IAFSS.FSS.11-1326

O'Brien JJ (2017) Patterns and processes: Monitoring and understanding plant diversity in frequently burned longleaf pine (Pinus palustris) landscapes. Final Report, RC-2243.

O'Brien JJ, Hiers JK, Varner JM, Hoffman C, Dickinson M, Michaletz S, Loudermilk EL, Butler B (2018) Advances in mechanistic approaches to quantifying biophysical fire effects. Current Forestry Reports, 4, 161-177.

Ottmar RD, Hudak AT, Prichard SJ, Wright CS, Restaino JC, Kennedy MC, Vihnanek RE (2016) Pre-fire and post-fire surface fuel and cover measurements collected in the southeastern United States for model evaluation and development. International Journal of Wildland Fire, 25, 10-24. doi: http://dx.doi.org/10.1071/WF15092

Rothermel RC (1972) A mathematical model for predicting fire spread in wildland fuels. In. Intermountain Forest and Range Experiment Station, Odgen, UT: USDA Forest Service.

Rowell E (2005) Estimating Forest Biophysical Variables from Airborne Laser Altimetry in a Ponderosa Pine Forest, Master's thesis, South Dakota School of Mines and Technology, Rapid City, South Dakota, 99 p.

Rowell E, Loudermilk EL, Seielstad C, O'Brien JJ. (2016) Using simulated 3D surface fuelbeds and terrestrial laser scan data to develop inputs to fire behavior models. Canadian Journal of Remote Sensing, 42, 443-459.

Rowell EM (2017) Virtualization of fuelbeds: Building the next generation of fuels data for multiple-scale fire modeling and ecological analysis. Graduate Student Theses, Dissertations, &Professional Papers. 11115. https://scholarworks.umt.edu/etd/11115.

Rowell EM, Loudermilk EL, Hawley C, Pokswinski S, Seielstad C, Queen L, O'Brien JJ, Hudak AT, Goodrick S, Hiers JK (2020) Coupling terrestrial laser scanning with 3D fuel biomas sampling for advancing wildland fuels characterization. Forest Ecology and Management. 462:117945.

Schlager S (2017) Morpho and Rvcg–Shape Analysis in R: R-Packages for geometric morphometrics, shape analysis and surface manipulations. Statistical shape and deformation analysis (pp. 217-256).

Silva CA, Hudak AT, Vierling LA, Loudermilk EL, O'Brien JJ, Hiers JK, Jack SB, Gonzalez-Benecke C, Lee H, Falkowski MJ, Khoravipour A (2016) Imputation of individual longleaf pine (Pinus palustrisMill.) tree attributes from field and LiDAR data. Canadian Journal of Remote Sensing, 42:554-573. doi: https://doi.org/10.1080/07038992.2016.1196582

Tierney ML (2015). Package 'misc3d'.

Waldrop TA, Goodrick SL. (2012) Introduction to prescribed fires in Southern ecosystems. Science Update SRS-054. Asheville, NC: US Department of Agriculture, Forest Service, Southern Research Station. General Technical Report54: 1-80.

Walters JR., Daniels SJ, Carter III JH, Doerr PD (2002) Defining quality of red-cockaded woodpecker foraging habitat based on habitat use and fitness. The Journal of Wildlife Management: 1064-1082https://doi.org/10.2307/3802938.

Appendix A-Supplemental Data

A.1 Data Repository

All fire behavior input data are being transferred to the United States Forest Service Data Archive (https://www.fs.usda.gov/rds/archive/).

Table A.1. List of uploaded data files for the United States Forest Service Data Archive

Name	Format	Resolutions	Type
Pebble Hill Plantation	QUIC-fire; HIGRAD\FIRETEC Voxel GRID	2m – 4m – 8m -16m - 32m – Single	Bulk Density
Pebble Hill Plantation	QUIC-fire; HIGRAD\FIRETEC Voxel GRID	2m – 4m – 8m -16m - 32m – Single	Fuel Moisture
EAFB-L2F	QUIC-fire; HIGRAD\FIRETEC Voxel GRID	2m – 4m – 8m -16m - 32m – 64m	Bulk Density
EAFB-L2F	QUIC-fire; HIGRAD\FIRETEC Voxel GRID	2m – 4m – 8m -16m - 32m – 64m	Fuel Moisture

A.2 EAFB Fire Simulations and Input Data

A total of 54 runs were done using a laptop with 8 cores requiring almost 35 hours to run. Analysis scripts were then performed using Python and shell script commands taking another 2 hours. Due to the size of the domain and the overall length of the simulation being longer, ensemble runs. Fire behavior results showed distinct variation between environmental conditions and fuel resolution scales, with moisture level conditions having the least influence, and resolution scale having the highest. Results for fire behavior metrics are shown in Figure A.1 Fuel and moisture inputs for all scales are shown in Figure A.2.

***Figure A.1**: Fuel consumption at simulation end time for different resolutions for L2G Plot. Fuel resolution is a) 2m, b) 8m, c) 16m, d) 32m, e) 64m, f) single characteristic*

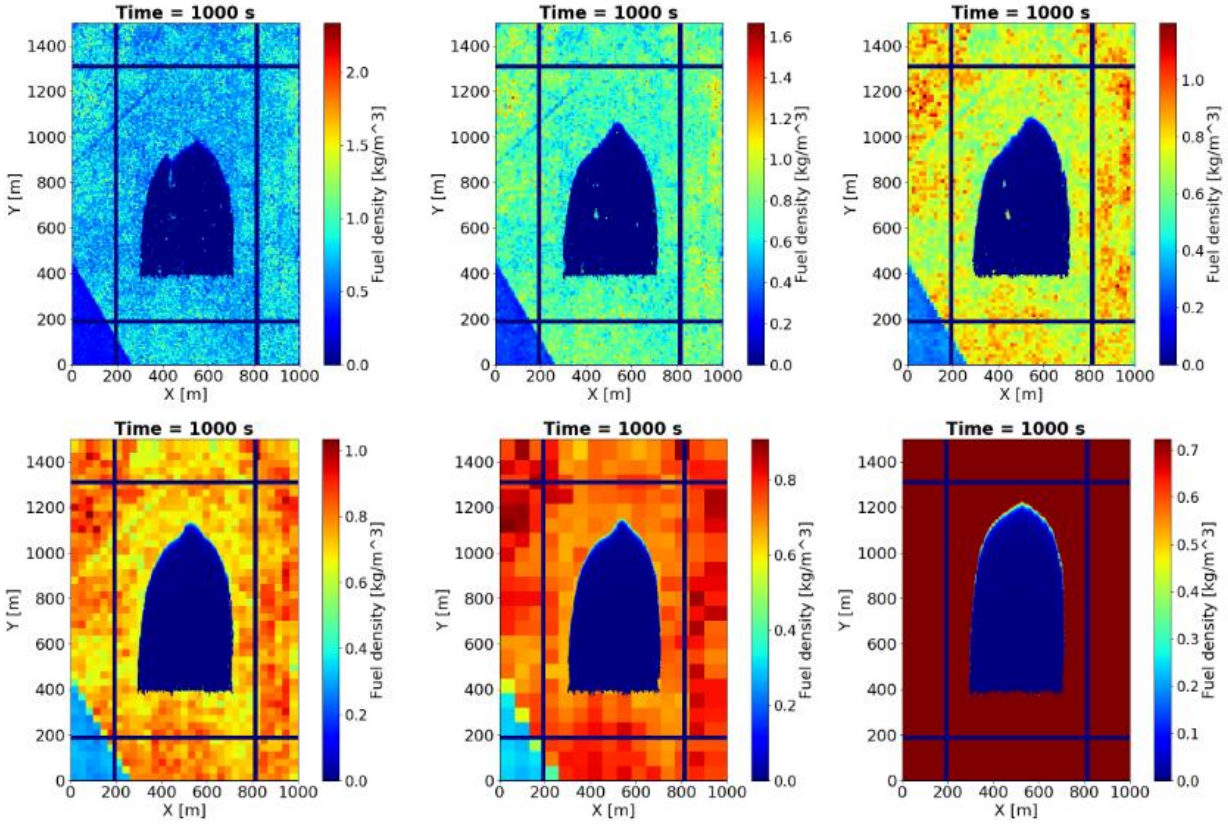

***Figure A.2**: Finished computational domain for L2G Plot.*

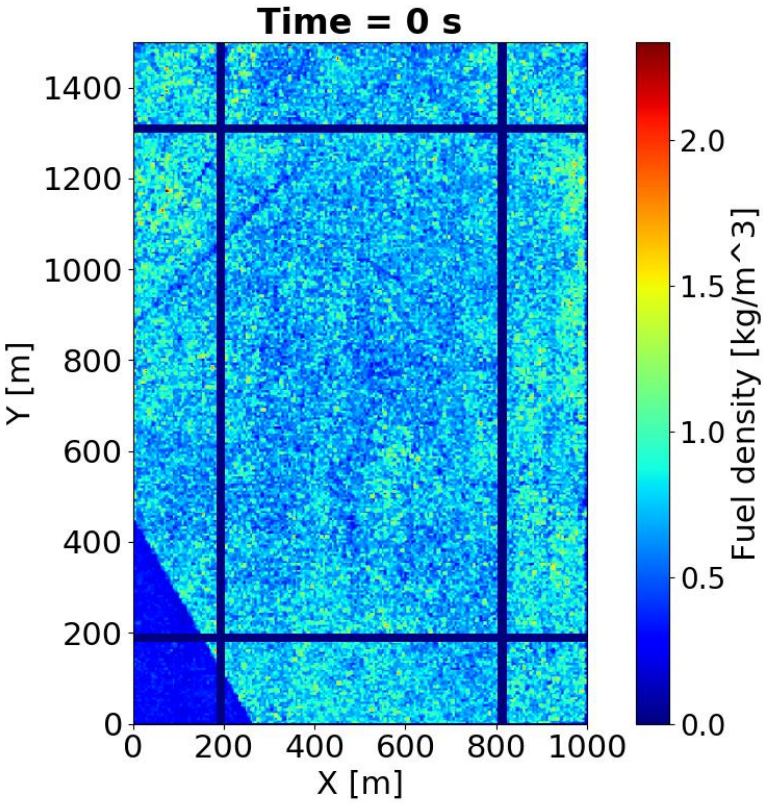

Figure A.3: Fuelbed characteristics at different resolutions for L2G plot

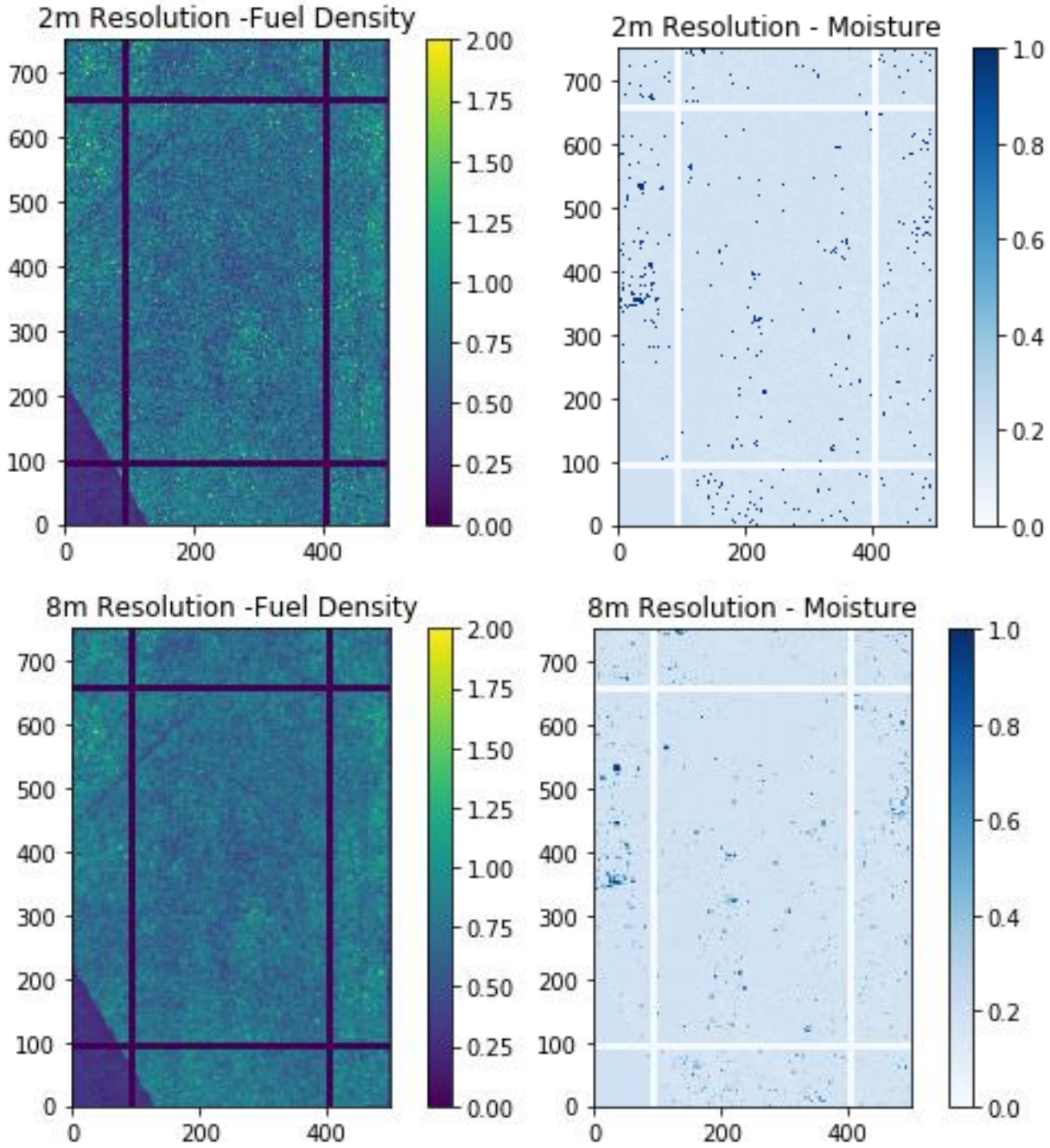

Figure A.3: *Continued*

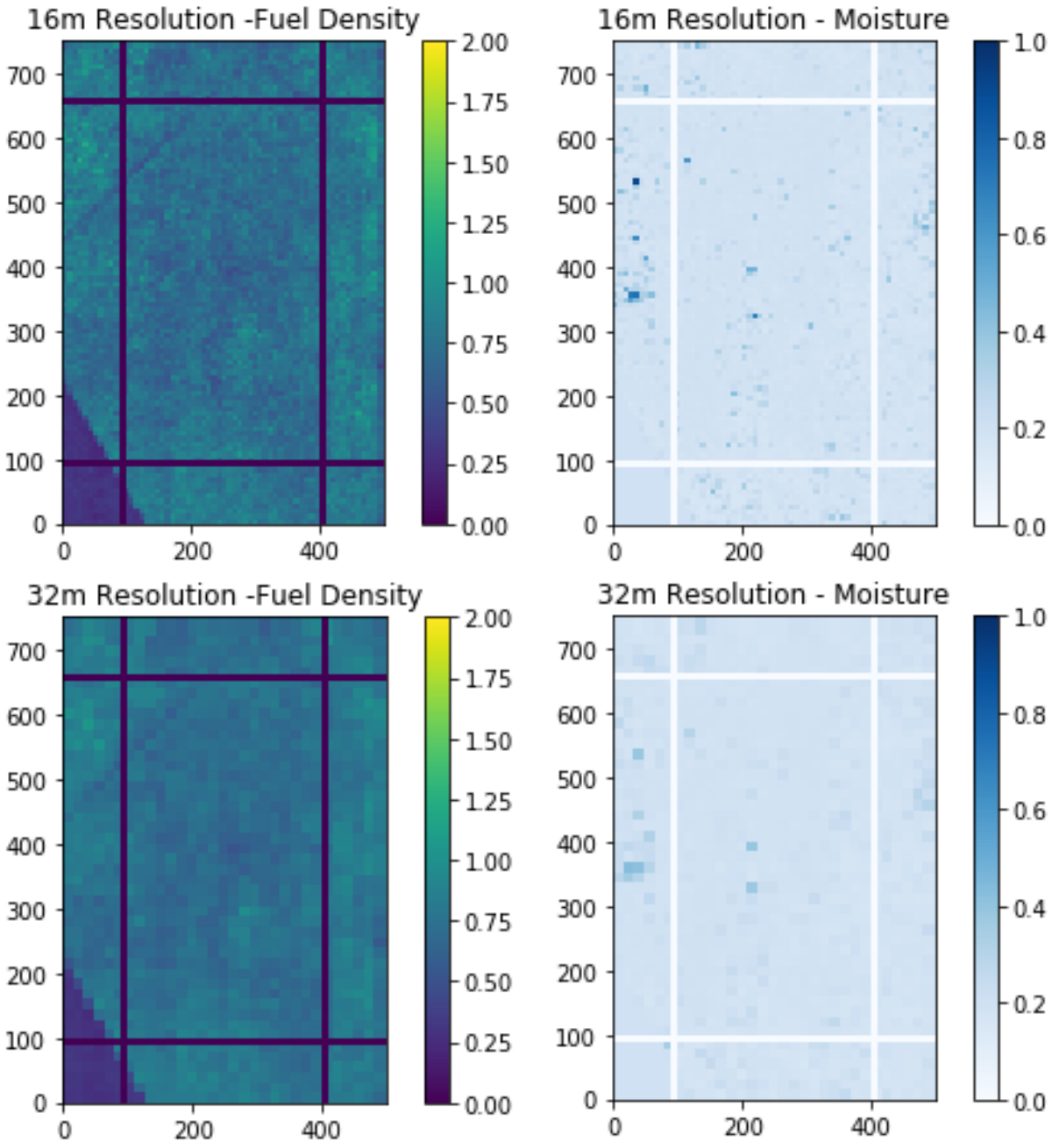

Figure A.3: *Continued*

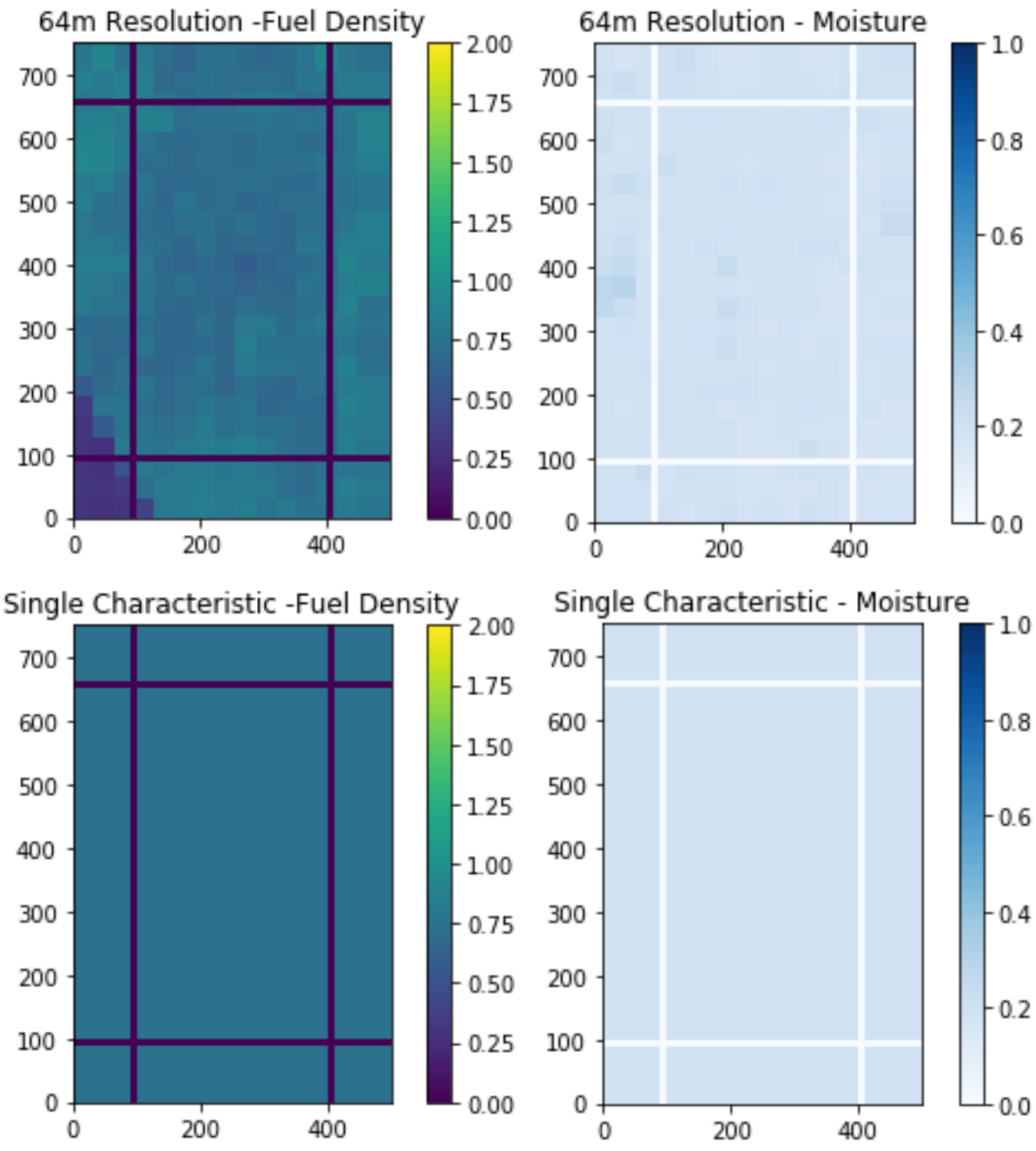

Appendix B-List of Publications

Appendix B.1 Peer Reviewed Journals

In Print:

Rowell EM, Loudermilk EL, Hawley C, Pokswinski S, Seielstad C, Queen L, O'Brien JJ, Hudak AT, Goodrick S, Hiers JK (2020) Coupling terrestrial laser scanning with 3D fuel biomas sampling for advancing wildland fuels characterization. Forest Ecology and Management. 462:117945.

In Preparation:

Rosales-Giron D, Hiers JK, Rowell EM, Loudermilk EL, Goodrick S (in prep) The influence of fuel heterogeneity on fire spread, planned submission November 2020 to Environmental Modeling & Software.

Appendix B.2 Theses

Rosales-Giron, Daniel (2020) A method of fuel characterization for fire behavior models and the influence of fuel heterogeneity on fire spread. Masters's Thesis, Department of Scientific Computing, Florida State University, Tallahassee, Florida.

Appendix B.3 Conference Abstracts and Presentations

Robinson R, Rowell E, Quaife B, Hiers K (2019) Calculating distributions of 3D litter layers with numerical simulations. American Geophysical Union, Fall Meeting, San Francisco, CA, 9-13 December.

Rosales-Giron D, Linn R, Hier K, Speer K, Quaife B (2019) Examining how ignition patterns control consumption of surface and canopy fuels using coupled fire-atmospheric models. American Geophysical Union, Fall Meeting, San Francisco, CA, 9-13 December.